Fourier-transform infrared spectroscopy for detection and quantification of polymer nano-particles

By

Kosta Milovanovic

B.A. University of South Florida, 2017

Thesis

Submitted in partial fulfilment of the requirements for the Degree of Master of Science in the Department of Biotechnology at Brown University

PROVIDENCE, RHODE ISLAND

MAY 2020

AUTHORIZATION TO LEND AND REPRODUCE THIS THESIS

As the sole author of this thesis, I authorize Brown University to lend it to other institutions or individuals for the purpose of scholarly research.

Date: _____ Signature: _____

Kosta Milovanovic, Author

As the sole author of this thesis, I further authorize Brown University to reproduce this thesis by photocopying or the means, in total or part, at the request of other institutions or individuals for the purpose of scholarly research.

Date: _____ Signature: _____

Kosta Milovanovic, Author

This thesis by Kosta Milovanovic is accepted in its present form by the Department of Biotechnology as satisfying the thesis requirements for the degree of Masters of Science.

Date:_____ Signature:_____

Dr. Edith Mathiowitz, Advisor

Date:_____ Signature:_____

Dr. Stacia Furtado, Reader

Date:_____ Signature:_____

Dr. Andrea Sobieraj, Reader

Vita

Kosta Milovanovic was born September 18th, 1995 to Jasmina Milovanovic and Ivica Milovanovic, in Belgrade, Serbia. His primary education was completed in Belgrade, Serbia. The Elementary and Middle school he attended is named Ratko Mitrovic after a national war hero. From there, he applied to a competitive newly formed Highschool named Računarska Gimnazija, where he got accepted. The school mainly focused on developing the students ability to code and operate computers at a high level. During his time as a student, he also competed competatively in Tennis.

After finishing Highschool, he applied and got accepted to the University of South Florida, in Tampa, Florida. There he applied himself in the field of biocehmistry and chemistry, earning a bachelors in Biomedical Sciences. While attending Univeristy of South Florida, he continued to be a part of the tennis comunity, running as the Vice President of the tennis on campus club.

From there, he applied to graduate programs which focused on biotechnology, and enrolled at Brown University as graduate student in the Department of Biotechnology. He interviewed with Dr. Edith Mathiowitz, and joined her team to help in the developement of polymeric nanoparticle delivery systems. In the Mathiowitz lab, his main focus was the detection of polymeric nanoparticles in tissue using FTIR spectroscopy. After graduation, he will focus on continuing his work in advancing technologies for treating human diseases and dissabilities.

Abstract of Fourier-transform infrared spectroscopy for detection and quantification of polymer nano-particles by Kosta Milovanovic, May 2020

Oral delivery of biologics is an extremely researched topic due to its possible benefits. One of the common ways to achieving this goal is by encapsulating proteins and nucleotides inside polymeric nanoparticles, which would protect the drug, and delivery it to its target location. Therefore, confirming nanoparticle presence within cells, and calculating bioavailability of nanoparticles is important to furthering research into this topic. Currently, most methods for identifying and quantifying nanoparticle presence within tissue are either cost prohibitive or time consuming. A novel approach to solving issues related to detection and quantification is the implementation of an FTIR spectrometer. The process of analyzing samples through a spectrometer is quick, simple and cheap. By creating control samples of tissue and polymer spectrums, and then combining samples to see if polymers could be identified within tissue *ex-vivo*, this research was successfully able to identify nanoparticles within tissue samples using an FTIR. Building upon that, calibration curves were made using the same *ex-vivo* approach, which were utilized within *in-vivo* experiments to successfully calculate bioavailability of nanoparticles fed to live rats. Ultimately, this project showed the viability of using an FTIR spectrometer to identify polymeric nanoparticles within tissue, and calculate the bioavailability of those nanoparticles.

Acknowledgements

First and foremost, I would like to thank my family, Jasmina Milovanovic, Ivica Milovanovic and Iva Milovanovic for supporting me through my academic journey. The path was not always easy nor simple, but they stood by me during difficult decisions. I would additionally like to thank my grandparents and my aunt who also stood by me and helped me in any way they could. A special thank you also goes to Dr. Edith Mathiowitz who showed incredible patience and compassion during my first real laboratory experience. Next, I would like to thank all my lab peers and guides who assisted me in my project and in the writing of the thesis. All of this could not have happened without the full support Brown University has showed over the last two years so I would like to thank all the administrative staff who kept me in line with the deadlines and answered any questions and concerns I had during this process.

Table of Contents

Table of Figures

Table of Tables

Background

Most of pharmacology since the discovery of penicillin has been focused on organic chemistry and the discovery of low molecular weight therapeutics. These agents, while useful in the range of therapies they treat, can be limited by pathways they target. To overcome the limitations associated with low molecular weight drugs, an emphasis has been placed on developing polypeptides and polynucleotides as medications. Oral delivery of protein and other biological agents has been sought after since the introduction of high molecular drugs into the pharmacological supply chain. Several difficulties arise when trying to formulate oral polypeptide and polynucleotide medications. The main difficulties lie with the harsh environments of the stomach and gastrointestinal tract, which are lined with enzymes, bacteria, and acidic environments. Additional complications arise when considering the penetration of the epithelium by these high-molecular weight drugs as well as the first pass through the liver. In a paper published by Morishita and Peppas they state “The main reasons for the low oral bioavailability of biologicals are presystemic enzymatic degradation and poor penetration of the intestinal membrane”.

A potential solution to these problems is the incorporation of nanoparticles into the equation. Biodegradable nano-particles have been researched intesnviely for the purpose of delivering drugs through harsh environments, acting as protective membranes. In a paper published by Hans and Lowman, they state “In particular, this class of carrier holds tremendous promise in the areas of cancer therapy and controlled delivery of vaccines”. Several biodegradable polymer nanospheres have been developed to specifically survive these harsh

environments. In a paper published by Mathiowitz et al, they state “engineered polymer microspheres made of biologically erodible polymers, which display strong adhesive interactions with gastrointestinal mucus and cellular linings, can traverse both the mucosal absorptive epithelium”. Combining biologics with polymer nanoparticles could provide a more effective and convenient way of administering treatment to patients.

While Mathiowitz et al showed that polymeric nanoparticles can penetrate the epithelium using TEM and gold embedded nanoparticles, a faster method needs to be developed to both show penetration and identify percent uptake within *in-vivo* studies. Previous research in the Mathiwitiz lab focused on testing whether a Fourier-Transform Infrared-Spectrophotometer could be used to identify the presence of different polymers within gastrointestinal tissue. Specifically, the research mainly involved testing several polymers, including polystyrene (PS), poly(butadiene-maleic anhydride-co-L-DOPA) (PBMAD), poly-lactic acid (PLA), poly-fumaric-co-sebacic acid, against excised GI tissue (Perez).

While this initial probe in developing a new technique for detecting polymers in tissue showed promise, several practical issues were left unresolved. First, polymer detection was only verified in GI tissue samples. This only indicates that the polymers penetrated the mucosal membrane and entered the epithelium. It does not make any conclusions as to whether the polymers penetrated through the epithelium and entered the blood stream, nor did it show any results as to the percent uptake of those polymers. Additionally, the focus of the previous research relies on polystyrene, a non-biodegradable polymer which could be toxic to animals as well as humans due to their accumulation in the body (Lu et al). Therefore, the main objective of this project is to expand on the polymers detectable in tissue using the FTIR spectrometer

method, focusing on biodegradable and safe for human consumption polymers, as well as attempt to calculate percent uptake of nanoparticles using said method.

Because the project was designed to build upon previously achieved goals, this thesis was designed to reflect the process of the research itself. Therefore, the thesis is setup as a series of three consecutive Aims, which builds upon the previously discussed topic. Those three Aim are:

Aim I – The detection of new polymers in blood and tissue.

- This Aim will focus on detecting new polymers in GI tissue, as well as attempting to detect a polymer in blood.

Aim II – The creation of calibration curves for the detected polymers in the chosen tissue.

- This aim will focus on creating calibration curves for the detected polymers in GI tissue, as well as creating a calibration curve for PLA in blood plasma.

Aim III – *In-vivo* experiments designed to test the flexibility of the previous two aims, and an attempt at calculating biouptake of polymers using the created calibration curves.

- This aim will focus on testing whether detection can translate into an *in-vivo* experiment and calculating the polymer percent and biouptake if detected.

Each of the three Aims will contain an experimental section and a discussion/conclusion section.

Materials:

Because the project is designed to create a novel method for nanoparticle detection which is cheaper and faster, most of the materials will be used during each aim. Therefore, only one material section will be written, which reflects the materials used in every Aim. All of the materials if not stated otherwise were provided by Fisher Scientific. The polymers were provided by Takeda for PLA, and PFASA was made in-house.

To run the samples through the FT-IR, they first need to be mixed with KBr and made into a thin pellet. To do so, the following equipment was used: Non-electrostatic grinding bowl, Non-electrostatic grinding tool, Precise Scale in a low humidity environment (up to 0.05mg precise), non-electrostatic weighing paper, Scoopula, Razor Blade, Pellet press including individual parts, FT-IR Spectrometer, Computer for analysis, Rat tissue, PLA polymer, Fumaric Acid Monomer, laboratory grade KBr.

For the *in-vivo* experiment, additional surgical tools were required including: scalpel, DI water, surgical grade stitching rope, stitching scissors, LeuerLock syringe, 20 gauge needle, gauze, 1 mL vials, 3 mL vials, 10 mL vials, sleeping agent, euthanizing agent, warming pads.

Specific Aim I – Creation of spectrums for polymer identification.

The objective of the first aim was to expand which polymers could be detected *in-vivo* using the FTIR spectrometer. Previously, the Mathiowitz lab had successfully identified peaks

for PS and PBMAD, and successfully created a calibration curve for PS. Due to polystyrene's nature of being a non-biodegradable polymer, the primary objective of this project was to test whether biodegradable polymers could be detected in Tissue using FTIR.

Poly-Lactic acid was chosen as the main polymer for this project due to it being both approved by FDA for several products, as well as being heavily researched for biological applications. To detect the polymer, initial scans of pure PLA and pure jejunum were done as controls. Then new samples were created of Jejunum spiked with PLA, to identify if PLA specific peaks appear on the spiked spectrograph. For the purpose of identifying polymers in tissue, it is important to select polymeric peaks which are not present tissue spectrographs. Therefore, any peaks marked as polymer-specific peaks found within the spiked samples would necessarily indicate polymer presence.

The second portion of Aim 1, after successfully identifying the presence of polymers in JEJ was to identify the presence of the same polymers in blood. The same method used to identify the presence of polymers in tissue can be used to identify the polymers in blood, blood plasma, or blood erythrocytes. This step is important for further proof of *in-vivo* polymer absorption. If the polymer nanoparticles penetrate the GI epithelium, they will be absorbed by the blood, and transported through the body. Providing evidence of polymer presence in blood will help with proving polymer absorption, and uptake.

In addition to visually scanning which peaks solely appear within the polymer spectrographs versus the tissue spectrographs, and vice-versa, peaks were also selected based on the known polymeric functional groups. For instance, PLA contains ester groups with a wavelength range between $1750cm^{-1}$ and $1730cm^{-1}$ when scanned using a spectrograph.

Alternatively, poly-fumaric-co-sebacic acid contains rapidly hydrolysable anhydride functional groups which tend to show a distinct peak in the 1818 cm^{-1} to 1750 cm^{-1} spectrograph wavelength range. Since ester and anhydride groups hydrolyze readily in aqueous environments, these peaks could be lacking in biological tissue, while being present in polymeric samples. Therefore, those peaks could be used to identify the presence of polymers in tissue.

Experimental Section:

Creating Control Images

The tissue samples were harvested from sacrificed rats. The GI was split into three segments (1:2:2 ratio) to distinguish between the Duodenum, Jejunum and Ileum. Each of the three segments were then transferred to 20 mL vials, flash frozen, and lyophilized for a week. The produced dry GI tissue was ground to a fine powder and transferred to a desiccator to minimize moisture contamination.

To collect the blood, control rats were sacrificed, and blood samples were collected in 1.5 mL pre-weighed vials. These vials were then centrifuged at 10,000 g for 8 min. This step separates the erythrocytes from the blood plasma. It is done to isolate the polymers in one of the two layers. The two layers were then separated using a micropipette and transferred to individual 0.5 mL vials. The vials were flash frozen and lyophilized for a week. The vials were then removed from the lyophilizer and transferred to a desiccator to reduce any moisture contamination till used for analysis.

The first step of the process was to create individual spectrographs for the polymers and the tissue. The FTIR spectrometer was capable of reading samples from a pressurized crystalline

pellet consisting of KBr and the desired sample. To create the pellet, a ratio of KBr to sample needs to be chosen. In order to obtain the sample pellets, a highly sensitive scale was used in a moisture-controlled environment. Each pellet was sensitive to the 0.05 mg level to ensure scan consistency. Once the appropriate amount of KBr and sample were weighed, they were transferred to a non-electrostatic mortar. The different materials then need to grinded and mixed together until a fine powder is produced. The powder is then placed within a pellet press under 10,000 kg of force for 15 min.

Once the pellets were created, they were carefully removed from the dye, and transferred to the FTIR spectrometer. A background scan was completed prior to, and the sample was scanned using 32 repeat scans with 1 cm^{-1} steps, and with a 4000-400 cm^{-1} range. The spectrograph file was then saved and transferred over to SpectraGryph for analysis.

This method was used to create both the control tissue, control PLA, PFASA, and fumaric monomer spectrographs. A ratio of 98:2 KBr:PLA, KBr:Tissue and 97:3 KBr:PFASA, KBr:Fumaric monomer in mg of weight was used for the creation of each pellet. For the blood plasma controls, a ratio of 99:1 KBr:Plasma was used.

Results and FTIR Analysis of tissue controls:

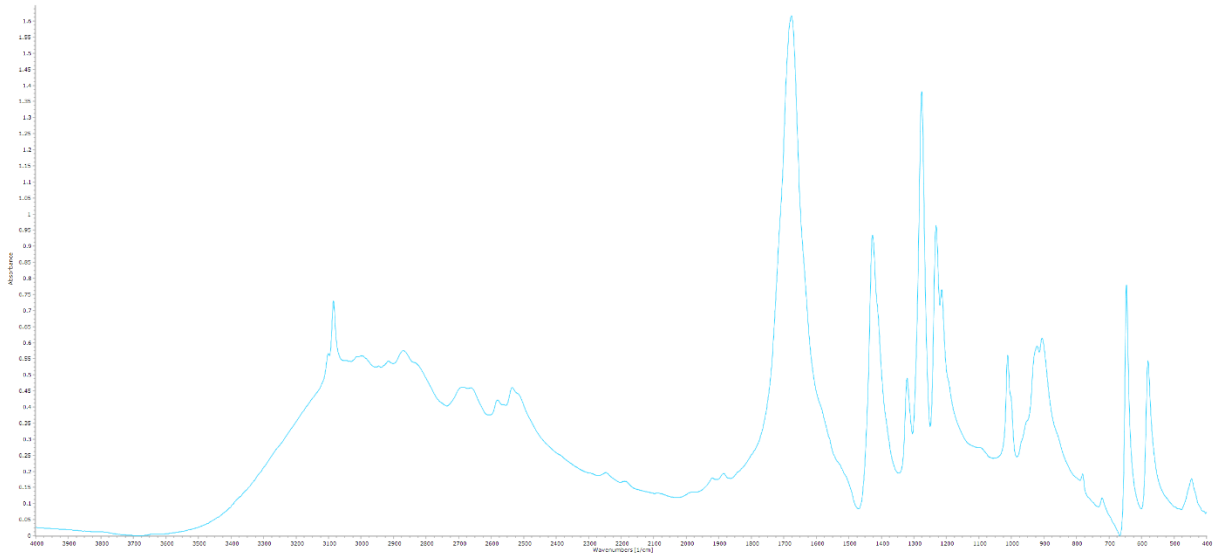

Figure 1 - Control scan of Fumaric Monomer. The pellet used for the scan consisted of 97 mg of KBr and 3 mg of Fumaric acid monomer. The software used to produce the spectrograph was SpectraGryph. The image was generated using 32 repeat scans with 1 cm^{-1} steps, and with a 4000-400 cm^{-1} range.

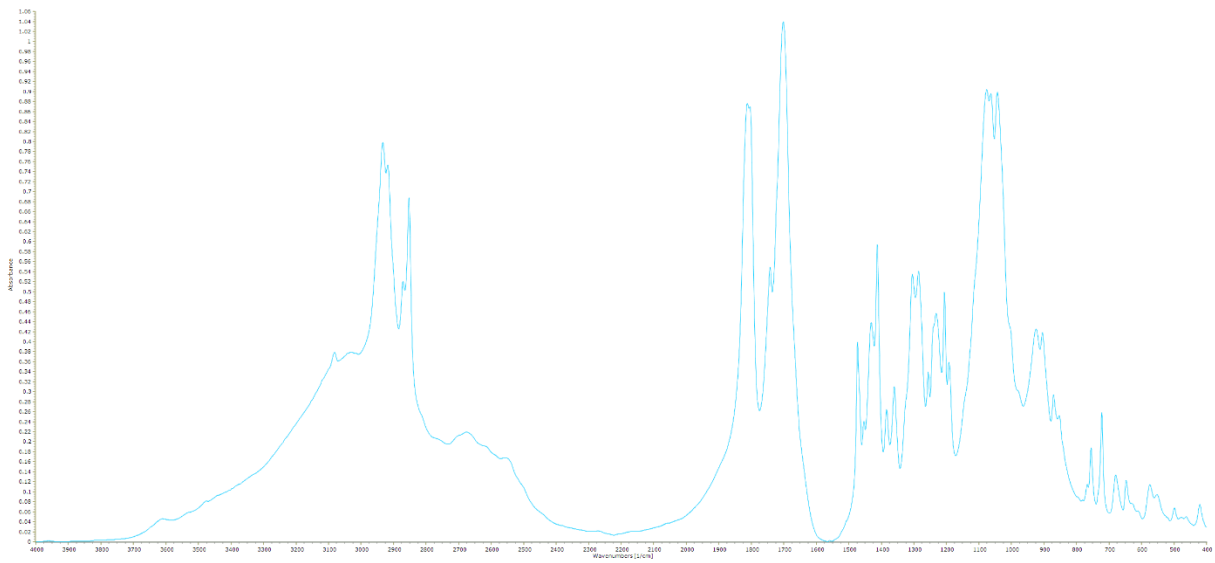

Figure 2 - Control scan of poly-fumaric-co-sebacic acid (PFASA). The pellet used for the scan consisted of 97 mg of KBr and 3 mg of PFASA. The software used to produce the spectrograph was SpectraGryph. The image was generated using 32 repeat scans with 1 cm^{-1} steps, and with a 4000-400 cm^{-1} range.

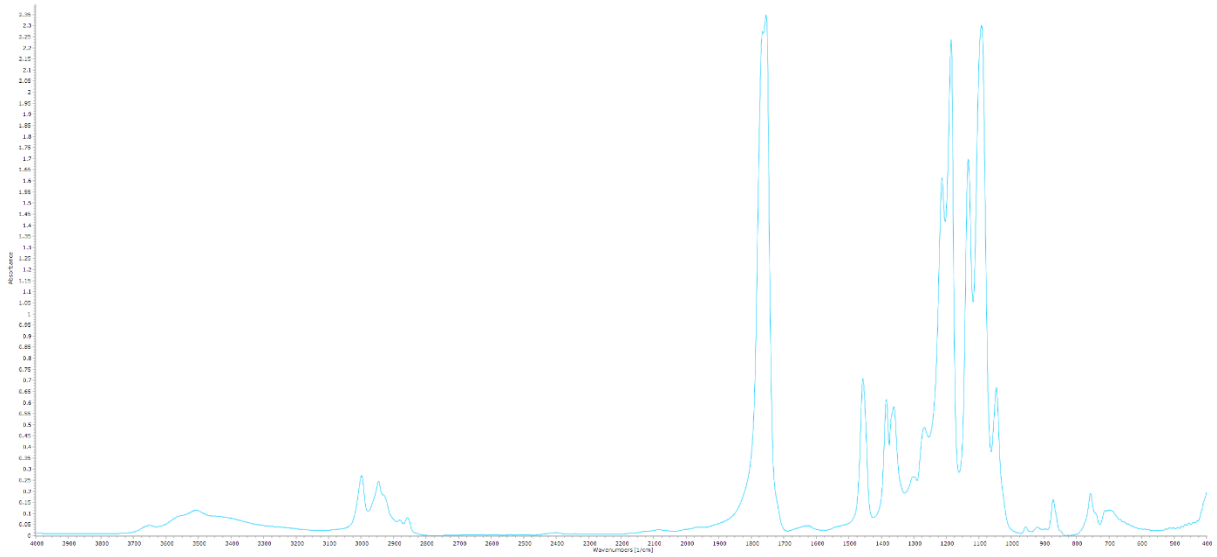

Figure 3 - Control scan of polylactic acid (PLA). The pellet used for the scan consisted of 98 mg of KBr and 2 mg of PLA. The software used to produce the spectrograph was SpectraGryph. The image was generated using 32 repeat scans with 1 cm^{-1} steps, and with a 4000-400 cm^{-1} range.

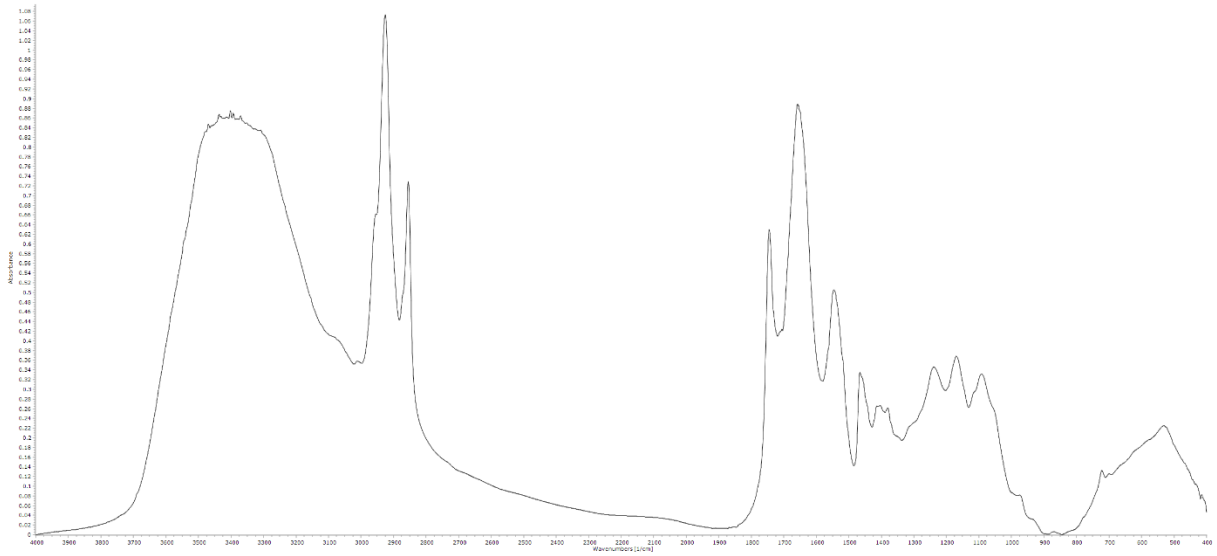

Figure 4 - Control scan of Jejunum (JEJ) tissue. The pellet used for the scan consisted of 98 mg of KBr and 2 mg of JEJ tissue. The software used to produce the spectrograph was SpectraGryph. The image was generated using 32 repeat scans with 1 cm^{-1} steps, and with a 4000-400 cm^{-1} range.

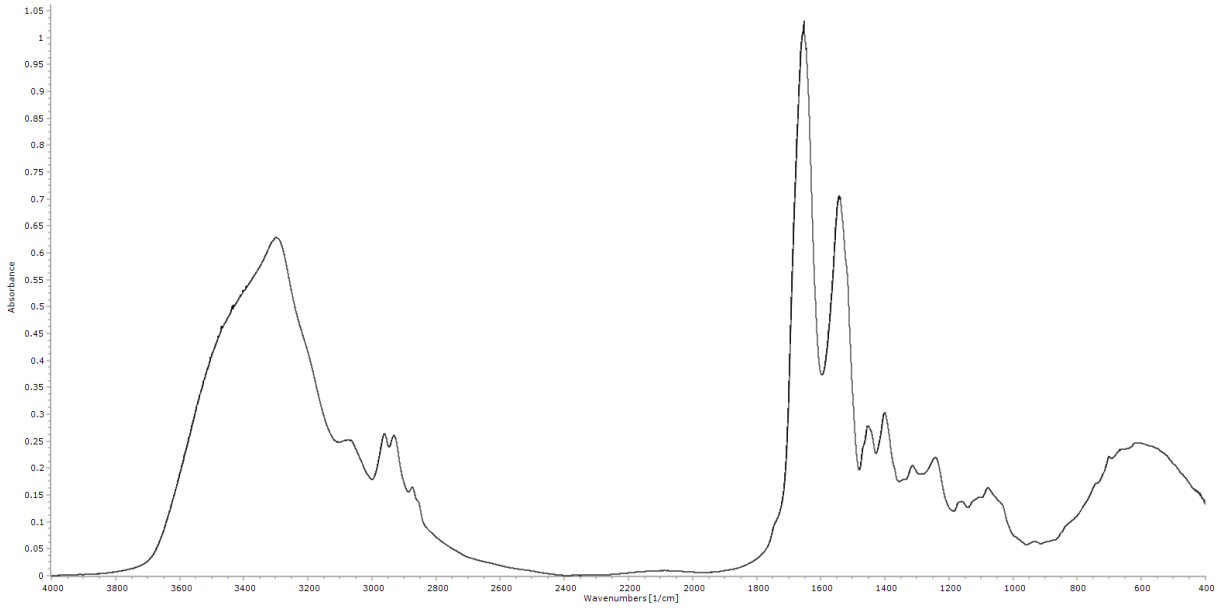

Figure 5 - A spectrograph of the sample made from blood plasma. The sample was made using the liquid method and was conducted to create a control of blood tissue. The sample pellet was made from 99 mg of KBr and 1 mg of blood plasma. The image was generated using 32 repeat scans with 1 cm^{-1} steps, and with a 4000-400 cm^{-1} range.

Figures 1-4 depict control spectrographs generated using the method described in Aim 1 Methods. Controls are spectrographs that contain only one samples, and not a mixture. Controls include pure polymer spectrums and pure tissue spectrums. All the images were created using the same FTIR spectrophotometer, imaging technique, and were analyzed in the same third-party software called SpectraGryph. Processing of the images consisted of a simple linear baseline tool present by default in the software. The baseline tool was used for each spectrograph sample used in this project.

As stated in the introduction, the main goal of Aim 1 is the identification of polymers within biological tissue. The idea is that a unique polymer peak not present in tissue would appear in spiked samples and confirm the presence of the polymer. Therefore, for a unique polymer peak to appear, a polymer must contain a peak not present in regular biological tissue. As biological tissue consists of many different proteins, poly-nucleotides and enzymes, most

functional groups should be present in an FTIR spectrograph. Groups with a low likelihood of appearing in tissue samples are ones that hydrolyze easily. These groups should technically degrade quickly in aqueous environments and without stabilizers, and not appear in FTIR spectrographs. Therefore, polymers with hydrolysable groups have the highest chance of containing peaks not present in tissue.

Figure 4, a spectrograph obtained by running a pure Jejunum tissue sample through an FTIR spectrophotometer, shows a multitude of peaks expected to be present in biological tissue. Particularly, the most prevalent peaks shown in the spectrographs are in the 1600 cm^{-1} region, and can be attributed to amide bonds, the building blocks of proteins. When analyzing the graphs, the regions which seem to lack peaks are the 2800-1760 cm^{-1} region and the 970-630 cm^{-1} region. Other tissue spectrograph regions where the peaks take a downward thrust or in so called "valleys" could also be considered as suitable candidates to detect polymeric peaks.

As described in Aim 1 introduction, PLA has a few specific peaks. The structure of PLA is displayed in Figure 5. The C=O bond has a stretch at around 1750 cm^{-1} while the C-O bond has a stretch from 1210-1163. The C-O stretch at 1210-1163 cm^{-1} is also specific as it usually manifests in two close peaks, as shown in Figure 3. Both peaks correspond to the ketone functional group. As the ketone functional groups are the most prominent functional group on the PLA polymer and have a low chance of appearing in biological tissue, peaks stemming from ketones are most likely to be chosen as unique to the polymer. Choosing between the C=O peak at 1750cm^{-1} - 1730cm^{-1}, and the two peaks present in the 1210 cm^{-1} region depends on the peaks present in the tissue spectrograph (Paragkumar N, et al).

While both PLA and PFASA contain hydrolysable functional groups, they differ greatly both in stability as well as their peak location on an FTIR spectrograph. Poly-fumaric-co-sebacic

acid, as its name suggests, is a polymer created by a condensation reaction between sebacic acid and fumaric acid. The structure of PFASA is shown in Figure 5. The ratio of the two monomers dictates its physical properties. The poly-fumaric-co-sebacic acid used in this experiment, as listed in the materials section, contains 20% fumaric acid monomer, and 80% sebacic acid monomer. The specific composition of the polymer was chosen due to the effectiveness it displayed in the (Furtado et al) study. The two main functional groups on PFASA, both of which could generate unique PFASA peaks on an FTIR spectrograph, are the anhydride group, and the alkene group. Additionally, due to the highly unstable nature of the anhydride group, PFASA degradation by hydrolysis generates an additional function group of carboxylic acid. The wavelength locations of the functional groups on the FTIR spectrograph shown in Figure 2 are 1810 cm^{-1} for they C=O anhydride stretching, 1750 cm^{-1} for the second C=O anhydride stretching, and 1700 cm^{-1} for the C=O carboxylic acid stretching. Additionally, as seen in Figure 2, the alkene groups show a small C-H peak at a wavelength of 3080 cm^{-1} corresponding to its stretching. The disubstituted C=C alkene group present in PFASA shows a strong peak at 720 cm^{-1} corresponding to its bending.

Fumaric acid is one of the two substituents which make up PFASA. As seen in Figure 1, fumaric acid shares much of its peaks and functional groups. The structure of Fumaric monomer is shown in Figure 5. The fumaric acid molecule is comprised of two carboxylic acids, and one alkene group. Due to the structural changes which occur during the condensation reaction needed to form PFASA, the location and spectrum location of the alkene groups differ between the monomer and the polymer. Specifically, the carboxylic acid which results from the breaking of PFASA is not a conjugated acid, while the carboxylic acid present in fumaric monomer acts a conjugated acid. This difference equates to the fumaric monomer having an acid peak location at

1680 cm^{-1} as opposed to PFASA having a non-conjugated acid location at 1700 cm^{-1}. The alkene peak location of PFASA is shared with that of fumaric monomer.

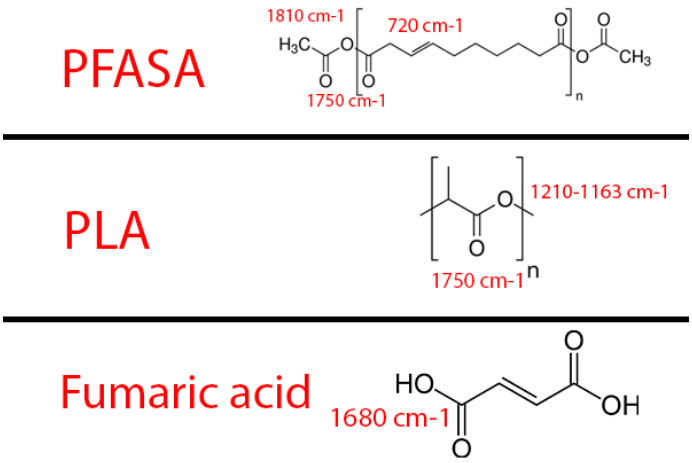

Figure 6 – An image showing the molecular structures of the two polymers and one monomer tested against tissue for detection, and for which calibration curves will be made. The numerical values next to the molecular structures represent the functional groups peak location on the spectrographs wavelength axis.

After the analysis of the control samples individually, the next step to identifying whether the selected polymers could be detected was to directly compare the polymeric spectrum files with that of the tissue sample. Figures 6-8 are generated in SpectraGryph with the aim of more easily comparing the tissue sample with that of the polymers. The tissue graphs in each figure is shown as orange, while the polymer sample is shown as blue.

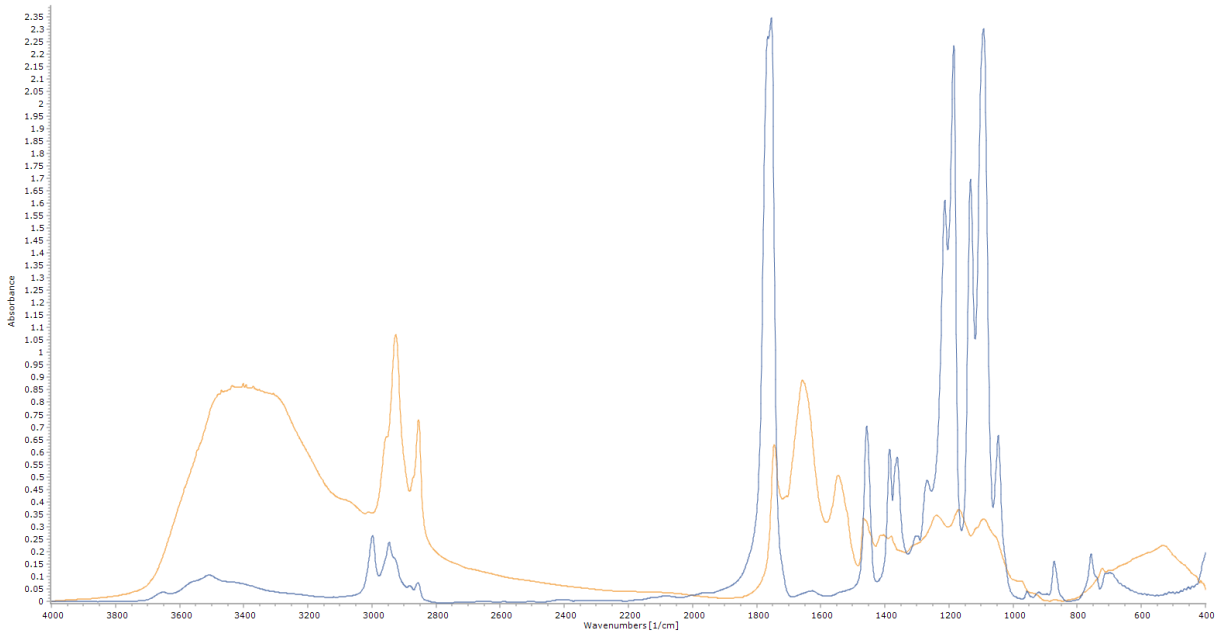

Figure 7 – Figure showing the spectrographs of PLA (shown in blue) and Jejunum tissue (shown in orange). The spectrograph is a visual representation of the two samples and shows peak differences between the two controls. Specifically, the 1750 cm^{-1} region of the PLA spectrograph shows a hard peak slightly shifted to the left of the tissue peak in the similar location. Additionally, the PLA spectrum shows peaks in the 1185 cm^{-1} region where two tissue peaks are separated by a "valley". The 1650 cm^{-1} tissue peak does not appear in the PLA spectrograph and could be thought of as unique to the tissue. Both the tissue and PLA spectrums were generated using the same methods described at the start of the results section.

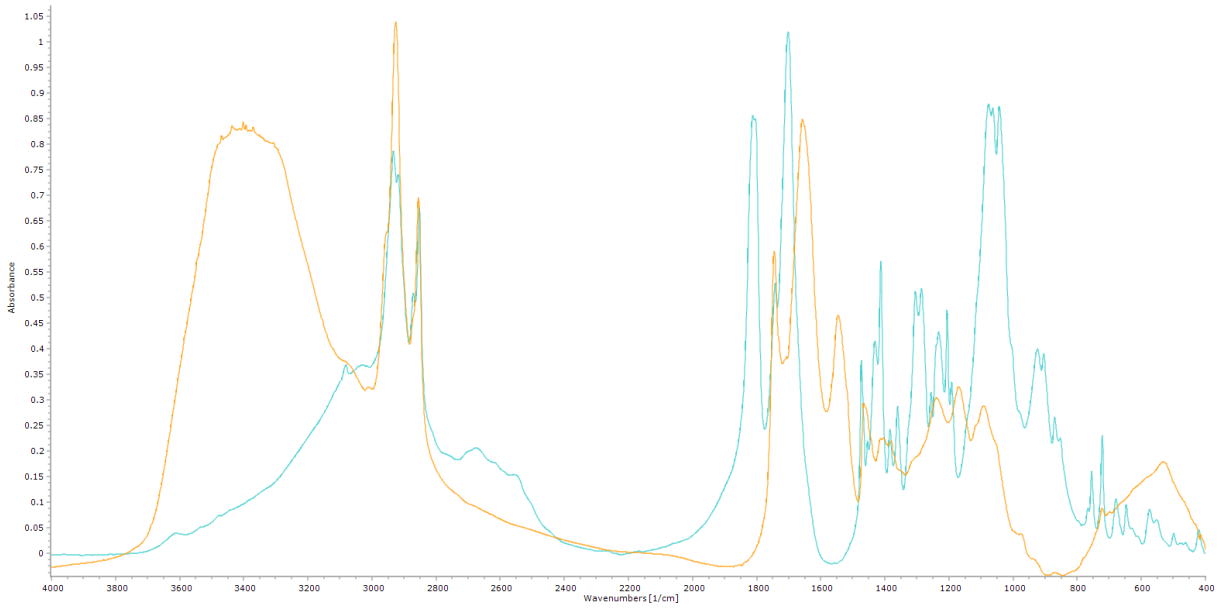

Figure 8 - Figure showing the spectrographs of PFASA (shown in blue) and Jejunum tissue (shown in orange). The spectrograph is a visual representation of the two samples and shows peak differences between the two controls. Specifically, the 1810 cm^{-1} region of PFASA shows a distinct peak not present in the tissue sample. Additionally, the PFASA spectrum shows peaks in the 720 cm^{-1} region where no tissue peaks are present. These two peaks could potentially be used to identify the presence of PFASA in tissue. The 1650 cm^{-1} tissue peak does not appear in the PFASA spectrograph and could be thought of as unique to the tissue. Both the tissue and PLA spectrums were generated using the same methods described at the start of the results section.

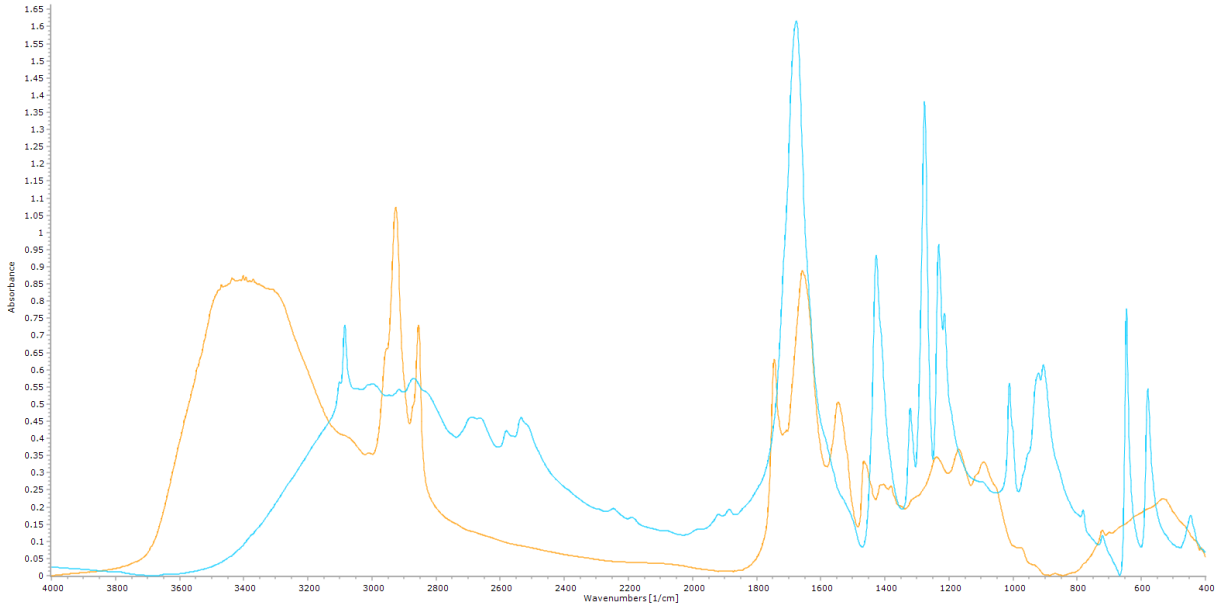

Figure 9- Figure showing the spectrographs of Fumaric Acid (shown in blue) and Jejunum tissue (shown in orange). The spectrograph is a visual representation of the two samples and shows peak differences between the two controls. Specifically, Fumaric monomer contains a sharp peak in the 3100 cm^{-1} regions which can be associated with the C-H bond of the alkene group. The broad peak of the fumaric acid's two carboxylic groups restrict it from being used for identification as it sits atop the two broad tissue peaks. The disubstituted binding of the C=C bond shows up in the 650 cm^{-1} region, where no tissue peaks are located. The tissue sample has a unique peak in the 1550 cm^{-1} region, unique to the tissue alone. Both the tissue and PLA spectrums were generated using the same methods described at the start of the results section.

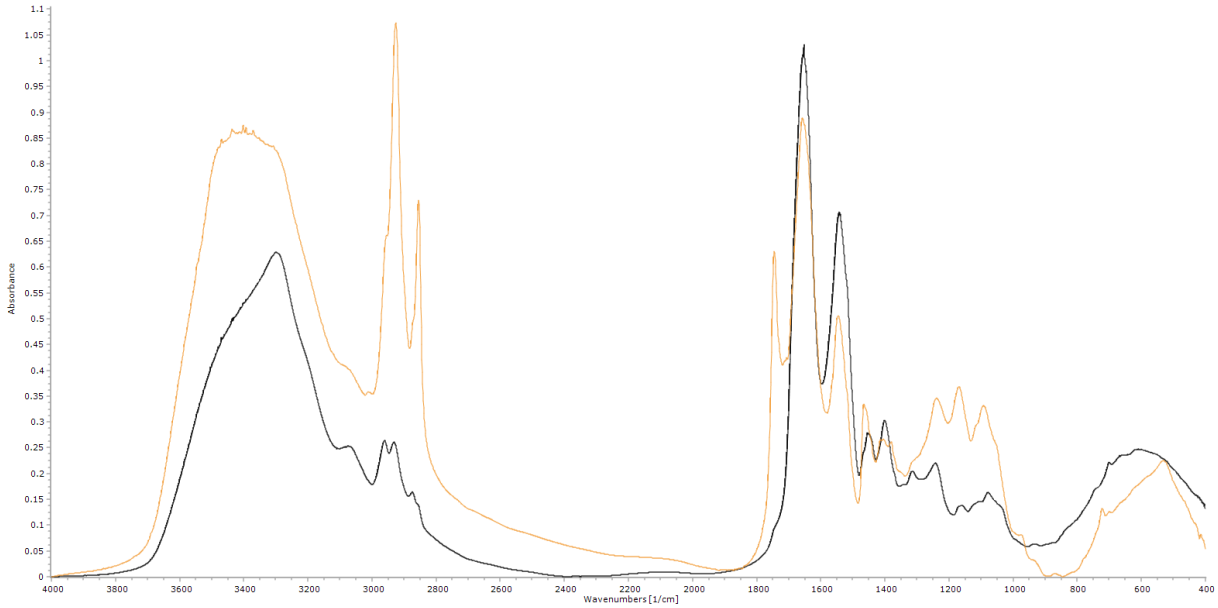

Figure 10– Figure showing Jejunum tissue (shown in orange) and blood plasma (shown in black). The image was generated to show the difference between two tissues in which polymer detection could apply. The main visible difference is in the 1750 cm^{-1} region where JEJ shows a distinguishable peak, and where no peak is present in blood plasma. Most other peaks are shared between the two spectrographs. Both tissue spectrums were generated using the same methods described at the start of the results section.

When comparing the polymers and the tissue spectrums atop one another, as seen in Figures 7-9, it becomes clear which peaks could be used for polymer detection. Specifically, both the 1750 cm^{-1} and the 1185 cm^{-1} peaks could be used to verify the presence of PLA, since no tissue peaks are present in those two regions. The 1810 cm^{-1} and 720 cm^{-1} could be used to identify the presence of PFASA in JEJ tissue. And the 3100 cm^{-1} and 720 cm^{-1} peaks could be used to identify the presence of Fumaric acid in tissue. Figure 10 was made to compare the two different tissues which were used for the project. Specifically, the black graph was made from the blood plasma sample spectrum, while the orange graph was made form the Jejunum tissue sample. The only significant difference between the two graphs was the presence of a peak in the JEJ sample at the 1740 cm^{-1} region, commonly associated with C=O bonds. Due to the similarities between JEJ tissue and blood plasma, all the listed peaks for each polymer could be used to identify the said polymer in blood plasma.

Once the controls were made, artificially spiked samples were created to see whether polymer specific peaks could be detected in tissue using the FTIR spectrometer. The method for creating these spiked samples is described at the end of the method section. The spiked samples were made using Jejunum tissue and the two listed polymers, PLA and PFASA and the one listed monomer, Fumaric acid. Figures 11-13 show the changes that occurred to the tissue spectrographs after they were spiked with either PLA, PFASA or Fumaric acid.

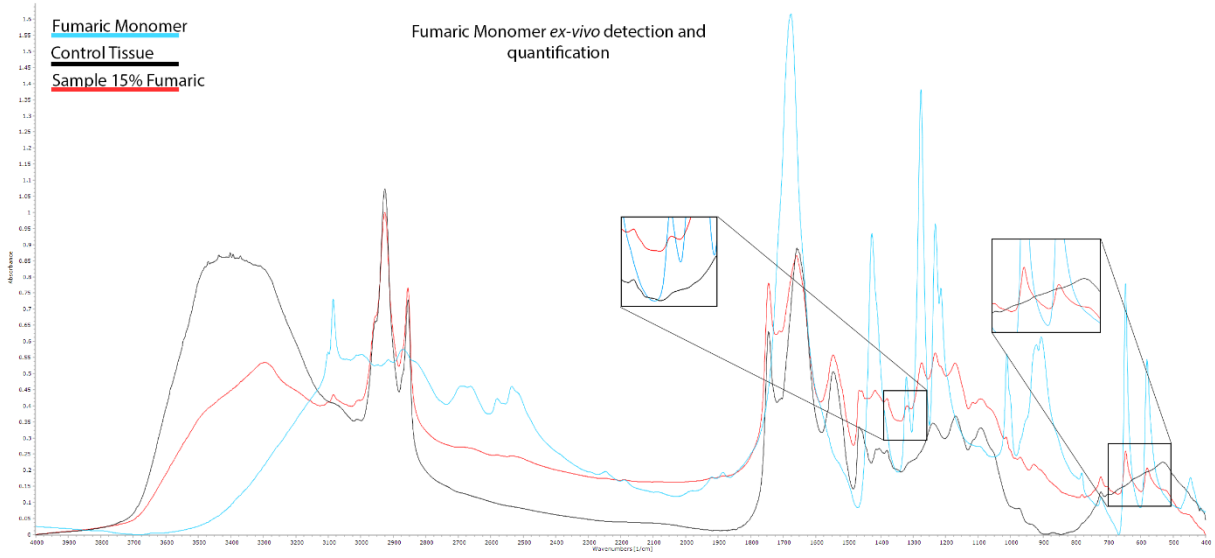

Figure 11– Graph showing the spectrum data of three samples. Red represents the Sample which consists of Fumaric monomer 15% and JEJ tissue 85%. Black represents the control JEJ tissue. Blue represents pure Fumaric monomer. The magnified regions show areas where the sample (red) is changed compared to the control tissue (black). These changes are attributed to presence of Fumaric acid within the sample pellet.

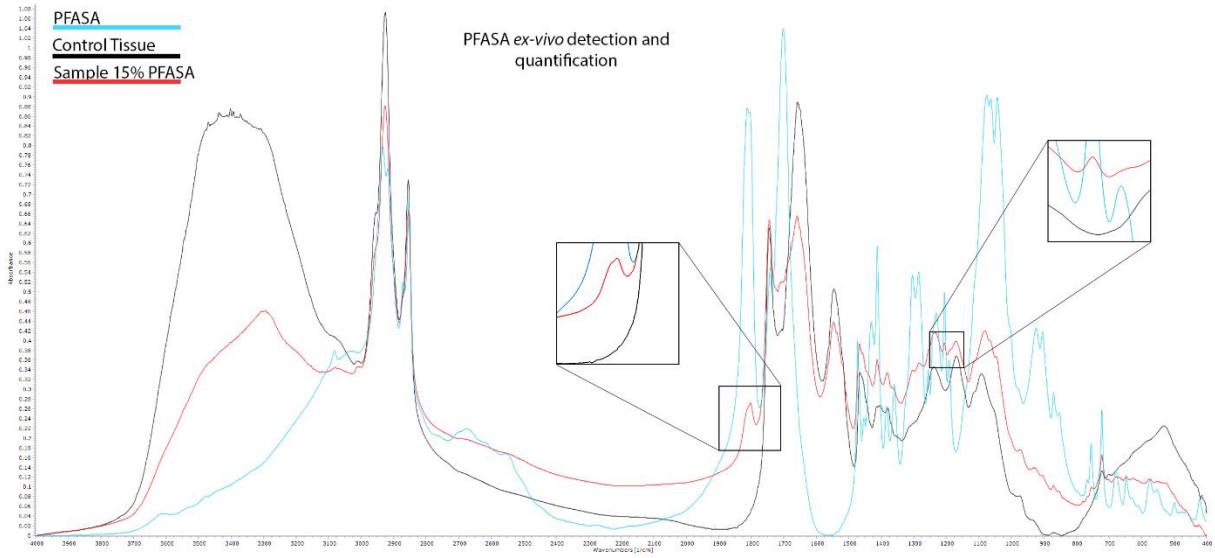

Figure 12- Graph showing the spectrum data of three samples. Red represents the Sample which consists of PFASA 15% and JEJ tissue 85%. Black represents the control JEJ tissue. Blue represents pure PFASA. The magnified regions show areas where the sample (red) is changed compared to the control tissue (black). These changes are attributed to presence of PFASA within the sample pellet.

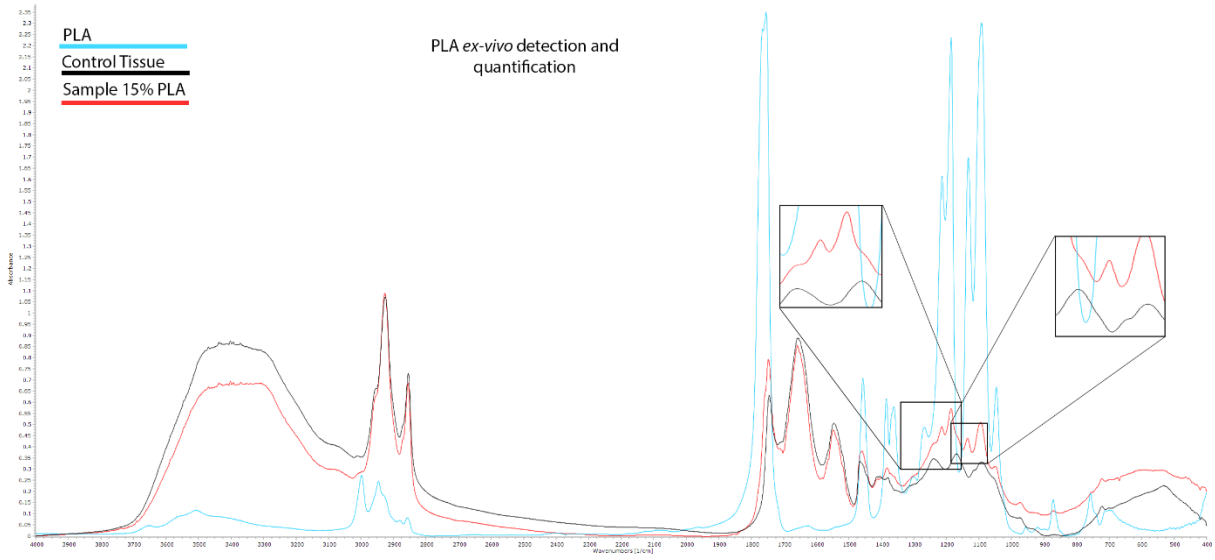

Figure 13- Graph showing the spectrum data of three samples. Red represents the Sample which consists of PLA 15% and JEJ tissue 85%. Black represents the control JEJ tissue. Blue represents pure PLA. The magnified regions show areas where the sample (red) is changed compared to the control tissue (black). These changes are attributed to presence of PLA within the sample pellet.

As seen in Figures 11-13, each spiked sample produced novel peaks not present in the control tissue spectrographs. The magnified regions of each figure show more detailed examples of the novel peaks. These peaks therefore prove that polymers and monomers can successfully be identified in tissue at concentrations of 15% and higher.

The identification of polymers within blood was done in a slightly different manner. Once the nanoparticles could be successfully detected in GI tissue, a simple experiment was conducted to see if the same could be done for blood. Initially, large concentrations of PLA were added to liquid non-dried blood, and these samples were flash frozen and lyophilized to create sample pellets. These samples showed no PLA presence in blood. The same experiment was then repeated, with the addition of separating blood into its plasma and erythrocyte components, as described in the method section. These separate components were again flash frozen and lyophilized, and made into sample pellets. The erythrocyte pellets showed no PLA presence, while the plasma pellet showed a slight peak in the 1750 cm^{-1} region of the spectrograph. Since it

was shown that unlike JEJ tissue, blood plasma contained no peak in that region, the new peak was attributed to PLA. Once PLA was shown to produce a slight peak in the described region, blood plasma was isolated from blood, and spiked using the same method as JEJ tissue. Figure 14 shows blood plasma spiked with PLA at a concentration of 85:15 Plasma:PLA.

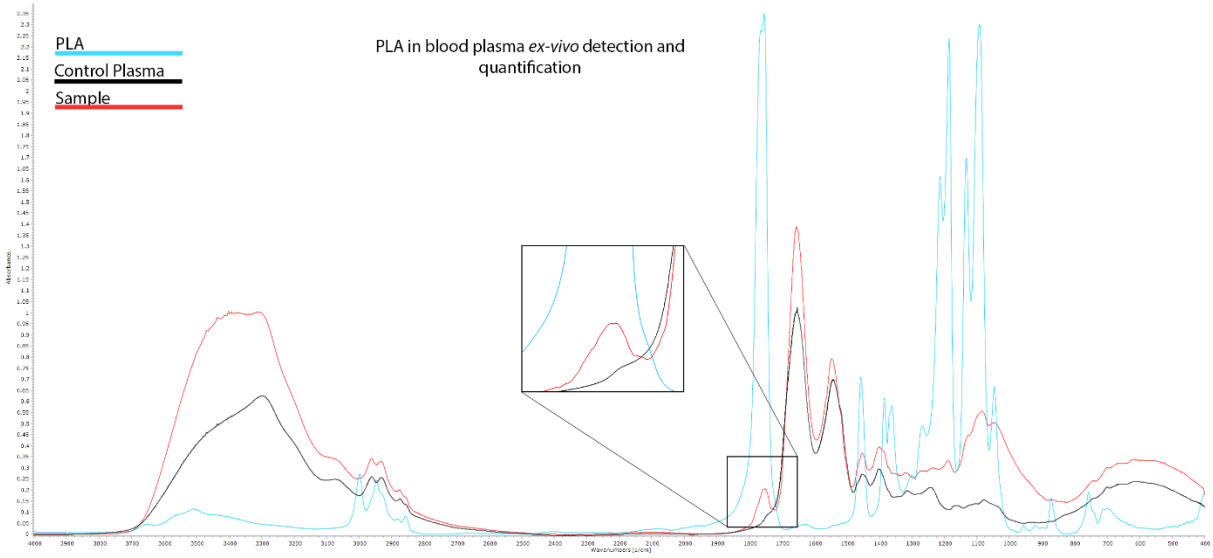

Figure 14- Graph showing the spectrum data of three samples. Red represents the Sample which consists of PLA 15% and blood plasma 85%. Black represents the control blood plasma. Blue represents pure PLA. The magnified regions show areas where the sample (red) is changed compared to the control blood plasma (black). These changes are attributed to presence of PLA within the sample pellet.

Conclusion:

The goal of Aim 1 was to test the new method of detecting polymers within tissue using an FTIR spectrometer, and possibly identify additional polymers which could be detected using this method. The way this was achieved was to first create control samples of tissue and polymer, and compare those to samples made with polymer spiked tissue. The hypothesis was that if new peaks which weren't present in the control tissue/blood samples appeared once spiked, those new peaks could be attributed to the added polymers.

As shown in figures 11-13, each polymer produced new peaks in the spiked samples not already present in the tissue sample. These peaks can therefore be used to identify the presence of polymers within JEJ GI tissue samples. Additionally, blood plasma was used as control in an additional experiment to see whether polymers could be detected in circulating blood as well. As shown in Figure 14, a novel peak was appeared in the PLA spiked sample which was not present in the blood plasma control. This peak is attributed to the strong C=O ketone peak prevalent in PLA. The presence of this peak in the spiked sample therefore shows that polymers and specifically PLA can be detected in circulating blood as well.

Specific Aim II – Creating a calibration curve, while focusing on interaction between polymer and tissue.

Experimental Section:

Creating tissue calibration curve samples:

Once the presence of polymers and monomers was confirmed in Aim 1, the next experiment was to see whether calibration curves could be made for the selected samples. The purpose of creating a calibration curve is to find a line formula for each polymer within the specified tissue. A line formula could then be used to identify an unknown amount of polymer or monomer within that tissue. With the help of a line formula, an *in-vivo* experiment can then be conducted in which a rat can be injected with polymer nanospheres, and the uptake of those nanospheres can be calculated.

A calibration curve was attempted for PLA, PFASA and Fumaric acid. The method for the creation of the calibration curve did not differ too much from the method used to spike the sample in Aim 1. Pellets were made with PLA concentrations in Jejunum tissue of 15%, 10%, 7.5%, 5%, 3.75%, 2.5% and 1% for PLA. For the fumaric acid monomer calibration curve, the following polymer/tissue concentrations were made: 15%, 10%, 7.5% and 5%. As with PLA, two additional pellets were made, pure Fumaric Acid, and pure Jejunum with mucus. Pellets with a PFASA concentration of 15%, 10%, 7.5%, 5%, 3.75%, 2.5% in JEJ-with mucus tissue were made.

The pellets were made by mixing the polymer/tissue sample with KBr. Specifically, a 98:2 ratio of KBr to sample ratio was used for PLA, while a 97:3 ratio was used for KBr to Fumaric acid, and KBr to P(FA:SA).

Since the total weight of the pellet equaled 100 mg, and PLA pellets contained 2 mg of sample and 98 mg of KBr, the difficulty with creating the calibration curves was the accuracy of the 2 mg samples. In general, the accuracy of the scale and the difficulty of transferring low weight samples limited the direct creation of the calibration curve points. For instance, a 5% PLA calibration curve point would require the transfer of 0.1 mg of PLA into the mortar. A mistake of 0.05 mg would equal a 5% error, which is too high for the accuracy and precision needed in this experiment. Therefore, a dilution method was used to create each calibration point for the JEJ tissue samples. This means that a larger batch of 15% sample was made, which was then diluted down to the required percentage points. This minimizes the starting point error, and since each new point required the addition of tissue and not polymer, it also reduced error in the lower percentage points.

The grinding of the PLA-Tissue mixture took between 25-30 minutes each. Since the grinding of the polymer-tissue mix made a sticky paste-like substance, and not an easily mixable powder, a scoopula was used to separate the mixture from the bowl, and then the mixture was grinded again. This was repeated approximately 5 times.

Once the mixture looked homogeneous, and no white spots were observed (which would indicate non-homogenous mixture), 2 mg were scooped up from the bowl and weighed on the precision scale. For this step, 2 ± 0.01 mg was ensured each time. The weighed mixture was then placed in the bowl containing 98 mg of pre-weighed KBr and both were grinded for approximately 15 min until visible homogeneity was achieved.

To create the Fumaric acid and P(FA:SA) samples, a slightly different procedure was used. Instead of mixing the tissue with polymer separately from KBr, all three materials were mixed together. This procedure reduced the amount of time needed to make a pellet, as it did not create a paste which stuck to the grinding bowl. The KBr ensured that both polymer and tissue mixed together in a powder form. The dilution method was still used to create the lower percentage points.

The Sample + KBr mixture was then transferred into the pellet making device and spread evenly using the scoopula. To ensure even spreading, the metallic cylinder was inserted, and rotated clockwise and counterclockwise 5 times. Once even spreading was ensured, the pellet making cylinder was placed into the press. The device was then set to 10,000 kg of pressure and maintained at that value for 15 min. The following table lists the values used to create each point on the concentration curves for PLA, Fumaric Monomer and P(FA:SA) calibrations:

Concentration Curve Values			
	PLA Concentration Curve	Fumaric Monomer Concentration Curve	P(FA:SA) Concentration Curve
15%	1.53 mg of PLA + 8.49 mg of JEJ-WM; 2 mg of mix pressed with 98 mg KBr	1.8 mg Fumaric Monomer + 10.2 mg of JEJ-WM + 388 mg of KBr mixed; 100 mg of sample Pressed	1.35 mg of P(FA:SA) + 7.65 mg of JEJ-WM + 291 mg of KBr mixed; 100 mg of sample Pressed;
10%	1.01 mg of PLA + 9.98 mg of JEJ-WM; 2 mg of mix pressed with 98 mg KBr	1 mg of Fumaric Monomer + 9 mg of JEJ-WM + 323 mg of KBr mixed; 100 mg of sample Pressed	1 mg of P(FA:SA) + 9 mg of JEJ-WM + 323 mg of KBr mixed; 100 mg of sample Pressed;
7.5%	1 mg of 15% sample mixed with 1 mg JEJ-WM; 2 mg of mix pressed with 98 mg KBr	50 mg of 15% sample mixed with 1.5 mg of JEJ-WM and 48.5 mg of KBr; 100 mg of sample Pressed	100 mg of 15% sample mixed with 3 mg of JEJ-WM and 97 mg of KBr; 100 mg of sample Pressed
5%	1.04 mg of PLA + 19.02 mg of JEJ-WM; 2 mg of mix pressed with 98 mg KBr	50 mg of 10% sample mixed with 1.5 mg of JEJ-WM and 48.5 mg of KBr; 100 mg of sample Pressed	100 mg of 10% sample mixed with 3 mg of JEJ-WM and 97 mg of KBr ; 100 mg of sample Pressed
3.75%	1 mg of 7.5% sample mixed with 1 mg of JEJ-WM; 2 mg of mix pressed with 98 mg KBr	N/A	50 mg of 7.5% sample mixed with 1.5 mg of JEJ-WM and 48.5 mg of KBr; 100 mg of sample Pressed
2.5%	1.03 mg of PLA + 39.02 mg of JEJ-WM; 2 mg of mix pressed with 98 mg KBr	N/A	50 mg of 5% sample mixed with 1.5 mg of JEJ-WM and 48.5 mg of KBr; 100 mg of sample Pressed
1%	0.51 mg of PLA + 49.51 mg of JEJ-WM; 2 mg of mix pressed with 98 mg KBr mix pressed with 98 mg KBr	N/A	N/A

Table 1 - This table lists all the numerical values used to create the concentration curves for PLA, Fumaric acid and P(FA:SA) in Rat Jejunum with Mucus. Specifically, it shows in mg how much of each substance was needed to create a 7 point curve for PLA, a 4 point curve for Fumaric monomer and a 6 point curve for P(FA:SA). The P(FA:SA) used had a 20:80 ratio.

After the pressing step was completed, the pellet was transferred to the FT-IR spectrophotometer within a plastic Ziploc bag. To run the spectrum and generate a spectrograph, a background scan was run first. Once the scan of the sample was complete, it was transferred to an SpectraGryph for further analysis.

Creating the blood plasma concentration curve samples:

The main difference between the creation of a tissue specific versus a plasma/blood specific calibration curve is the texture of the two materials. Tissue, and specifically the GI has a thick stretchy consistency even post lyophilization, while blood and plasma both turn into dissolvable powders post lyophilization. This property of blood plasma to turn into powder can then be utilized to create calibration curves in larger batches, while increasing accuracy and precision. The method for creating the plasma calibration curve was named the liquid method because it involves dissolving all three ingredients (Blood, KBr, and Polymer) into separate vials, and then mixing them in specific amounts to create the desired concentrations. Because P(FASA) rapidly dissolves in water, a calibration curve was not made for it using blood-plasma.

The liquid method involves the creation of three master vials with known concentrations of each substance. The solvent used in the creation of the PLA-blood calibration curve was water, since it dissolves KBr and plasma readily, and can diffuse PLA within its volume. From these vials, adequate volumes were withdrawn to create these concentration points: 1 %, 2.5 %, 5 %, 7.5 %, 10 %, 12.5 %, 15 %, 17.5 %, and 20 % and placed in individual vials. The tables below list the total mass and volumes for the master vials, and volumes withdrawn to create the individual vial curves:

Stock Solutions		
Sample Weight (mg)		**Water (mL)**
PLA	20	200
Serum	20	20
KBR	200	1

Samples	PLA (mL)	Serum (mL)	KBR (mL)	Sample Volume
20% Standard	3.0000	1.2000	0.7425	4.9425
17.5% Standard	2.6250	1.2375	0.7425	4.605
15% Standard	2.2500	1.2750	0.7425	4.2675
12.5% Standard	1.8750	1.3125	0.7425	3.93
10% Standard	1.5000	1.3500	0.7425	3.5925
7.5% Standard	1.1250	1.3875	0.7425	3.255
5% Standard	0.7500	1.4250	0.7425	2.9175
2.5% Standard	0.3750	1.4625	0.7425	2.58
1% Standard	0.1500	1.4850	0.7425	2.3775
Total Stock Volume	13.65	12.135	6.6825	

Table 2 - Table listing the values used for the liquid method in the creation of the plasma calibration curve. The top table lists the master vials with the amount in mg for the material used, and the amount of water in mL for the liquid used to disperse the material. The bottom table lists the volume of each solution used to create a single point on the calibration curve.

Once the individual point vials were filled with the correct volumes, they were vortexed and sonicated. This step ensures that all three components mix fully, and no clumps form. Once a vial was vortexed and sonicated, it was placed in liquid nitrogen to be flash frozen and transferred to the lyophilizer to fully dry.

Next, 100 mg is weighed out of each vial, and grinded in a non-electrostatic mortar and pestle. The ground powder was then transferred to a dye and pressed at 10,000 kg of pressure for 15 minutes. The pressed pellet was then extracted and scanned using the FTIR spectrometer.

Results and Analysis:

Tissue calibration curves:

Having confirmed the existence of polymer specific peaks within the polymer-tissue samples in Aim 1, the next step was to show that a reduction in concentration of polymer as compared to tissue would result in a smaller polymer specific peak. Modulating the reduction, a concentration curve could theoretically be made.

As shown in Figures 11-14, several polymer specific peaks can be used to create calibration curves for each of the chosen polymers. The selection of each is mainly subjective. Possible considerations include peak strength, peak area, peak specificity to the polymer etc. Additionally, a calibration curve can be created for many different peaks of the selected polymer, and the curves themselves can then be compared.

PLA has few specific peaks as described in the Analysis section of Aim 1. The C=O bond has a stretch at around 1750 cm^{-1} while the C-O bond has a stretch from 1210-1163 cm^{-1}. The C-O stretch is also specific as it usually manifests in two close peaks, as shown in Figure 3. These two peaks, specific for PLA are absent or much less pronounced in tissue, and therefore are suitable candidates for the calibration curve.

Since Tissue is comprised out of many different compounds, some overlapping peaks are to be expected between it and different polymers. As seen if Figure 7, where the pure PLA and Pure Tissue spectrographs are overlaid, Tissue peaks are present across a broad range of wavelengths. The tissue specific peak chosen for the PLA concentration curve, which does not manifest on the pure PLA spectrograph, was at around 1650 cm^{-1}.

Fumaric acid is also very specific for the carboxylic group at 1750 cm^{-1}. Unfortunately, as seen on Figure Y, tissue peaks show up at similar wavelengths making it difficult to construct a calibration curve for that peak. Fumaric acid also shows peaks at 1010 cm^{-1}, 850 cm^{-1} as well as 650 cm^{-1} and 590 cm^{-1}. All of these would be potential peaks for constructing a calibration curve.

Poly-Fumaric-co-Sebacic acid has several identifiable peaks, some of which show similarity to the peaks present in pure Fumaric Acid monomer (especially around the 650 cm^{-1} region). The primary identifiable peak of P(FA:SA) is the anhydride peak present around 1815 cm^{-1}. In Figure 12, the spike is present as a strong/sharp peak (Blue – 1812 cm^{-1}) and is absent from the tissue spectrograph (Black), and as such was chosen to be the polymer-specific peak. Several tissue peaks not present in the polymer spectrograph were available to choose from. From the list, the tissue-specific peak chosen was at 1650 cm^{-1}, as no P(FA:SA) spikes were present at that wavelength.

The main reason to identify tissue specific peaks, in addition to polymer specific peaks, is that concentrations for both the polymer and tissue change between different calibration curve points. When a polymer concentration decreases, the tissue concentration must increase. Since tissue has a presence at almost any polymer peak, a ratio needs to be created between tissue and polymer peaks to account for polymer peak decrease and tissue presence increase. If a ratio is not created, and polymer peak height was used as a pure data point for the calibration curve, it wouldn't account for tissue increasing peak height at that specific wavelength due to increase in tissue concentration. The ratio that is created from the standards for the polymer:tissue peaks then gives an approximate pure polymer decrease, and accounts for tissue increase for that specific wavelength.

Since PLA, Fumaric Acid monomer and P(FA:SA) all have different peaks, specific corresponding tissue peaks need to be selected for each. The tissue specific peak selected for PLA concentration curve was at 1650 cm^{-1}, while the tissue peak selected for Fumaric Acid monomer curve was at 1520 cm^{-1}, and the tissue-specific peak for the P(FA:SA) curve was at 1650 cm^{-1}.

Once the polymer specific and tissue specific peaks are selected, they can be extracted from the spectrograph samples created for each percentage point. The extracted data is generated from the peak heights and is measured by the absorbance strength of the peak. The spectrographs themselves were baselined using a simple linear baseline tool present in SpectraGryph. The charts with the extracted data are given below:

	1750 cm^{-1}	**1185 cm^{-1}**	**1650 cm^{-1}**
15%	0.70372	0.53223	0.59632
10%	0.79131	0.57122	0.85464
7.50%	0.96969	0.82771	1.395
5%	0.76159	0.56323	1.0211
3.75%	0.91822	0.70085	1.3451
2.50%	0.6982	0.44556	0.84766
1%	0.42231	0.3057	0.46811
0%	0.90689	0.68832	1.3336

Table 3 – Table listing the extracted absorbance data from the PLA calibration curve points. The data was extracted using SpectraGryph and was processed in Microsoft Excel. Each column lists the absorbance of the spectrograph at the specific wavelength. Each percentage points corresponds to the percent of PLA in the sample. The remainder of the sample was made from JEJ-WM. The 1750 cm^{-1} and the 1185 cm^{-1} points are attributed to PLA specific peaks while the 1650 cm^{-1} is attributed to a tissue specific peak.

	1812 cm^{-1}	723 cm^{-1}	1658 cm^{-1}
15%	0.27165	0.16528	0.65563
10%	0.21254	0.16109	0.6612
7.50%	0.23886	0.17164	0.59155
5%	0.226	0.17896	0.8048
3.75%	0.15	0.26415	0.98112
2.50%	0.08	0.16341	0.87881

Table 4 - Table listing the extracted absorbance data from the PFASA calibration curve points. The data was extracted using SpectraGryph and was processed in Microsoft Excel. Each column lists the absorbance of the spectrograph at the specific wavelength. Each percentage points corresponds to the percent of PFASA in the sample. The remainder of the sample was made from JEJ-WM. The 1812 cm^{-1} and the 723 cm^{-1} points are attributed to PFASA specific peaks while the 1658 cm^{-1} points are attributed to tissue specific peaks.

Wave	1010	650	580	1540
15%	0.3009	0.258	0.2071	0.5571
10%	0.2574	0.3274	0.2708	0.4768
7.50%	0.3195	0.3987	0.2801	0.6023
5.00%	0.2509	0.2969	0.2262	0.6379

Table 5 - Table listing the extracted absorbance data from the Fumaric acid calibration curve points. The data was extracted using SpectraGryph and was processed in Microsoft Excel. Each column lists the absorbance of the spectrograph at the specific wavelength. Each percentage points corresponds to the percent of Fumaric acid in the sample. The remainder of the sample was made from JEJ-WM. The 1010 cm^{-1}, 650 cm^{-1} and 580 cm^{-1} points are attributed to Fumaric acid specific peaks while the 1540 cm^{-1} points are attributed to tissue specific peaks.

As briefly explained at the introduction of Aim 2, a ratio of polymer peak to tissue peak must be created for the calibration curve. To make the ratio, each percentage point polymer specific peak must be divided from the same percentage point tissue specific peak. The were created in excel, and from those, the calibration curve points were finally created. The graphs below were created from those calibration curve points:

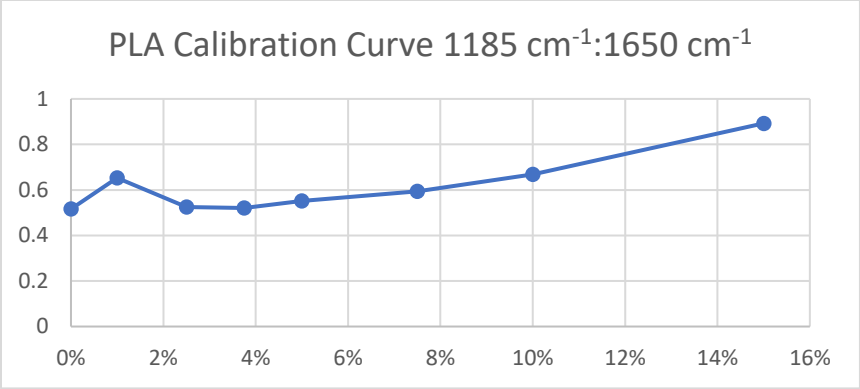

Figure 15 - Calibration curve created using 7 data points. The data points are made from samples created with PLA and JEJ tissue. Each decreasing percentage value is the result of lower polymer concentration within tissue. The Y axis is generated using specific polymer peak (at 1185 cm^{-1}) versus specific tissue peak (at 1650 cm^{-1}) absorbance ratios. The X axis corresponds to the percentage point of the generated ratio.

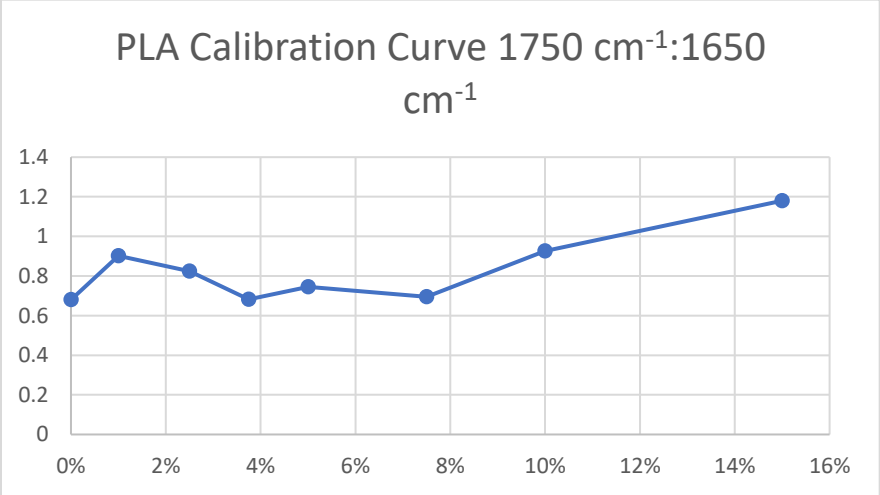

Figure 16 - Calibration curve created using 7 data points. The data points are made from samples created with PLA and JEJ tissue. Each decreasing percentage value is the result of lower polymer concentration within tissue. The Y axis is generated using specific polymer peak (at 1750 cm^{-1}) versus specific tissue peak (at 1650 cm^{-1}) absorbance ratios. The X axis corresponds to the percentage point of the generated ratio.

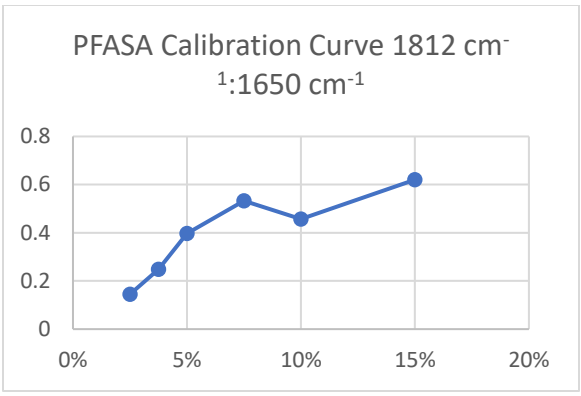

Figure 17- Calibration curve created using 6 data points. The data points are made from samples created with PFASA and JEJ tissue. Each decreasing percentage value is the result of lower polymer concentration within tissue. The Y axis is generated using specific polymer peak (at 1812 cm^{-1}) versus specific tissue peak (at 1650 cm^{-1}) absorbance ratios. The X axis corresponds to the percentage point of the generated ratio.

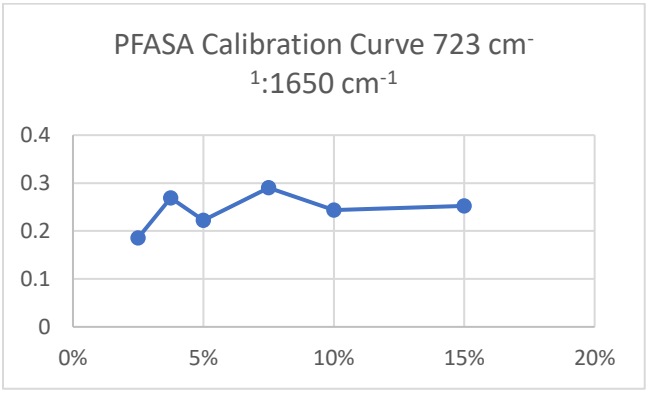

Figure 18- Calibration curve created using 6 data points. The data points are made from samples created with PFASA and JEJ tissue. Each decreasing percentage value is the result of lower polymer concentration within tissue. The Y axis is generated using specific polymer peak (at 723 cm^{-1}) versus specific tissue peak (at 1650 cm^{-1}) absorbance ratios. The X axis corresponds to the percentage point of the generated ratio.

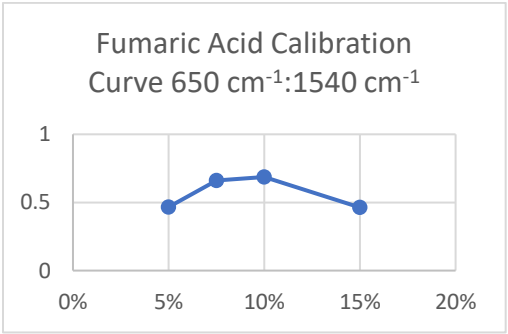

Figure 19 - Calibration curve created using 4 data points. The data points are made from samples created with Fumaric acid and JEJ tissue. Each decreasing percentage value is the result of lower polymer concentration within tissue. The Y axis is generated using specific polymer peak (at 650 cm^{-1}) versus specific tissue peak (at 1540 cm^{-1}) absorbance ratios. The X axis corresponds to the percentage point of the generated ratio.

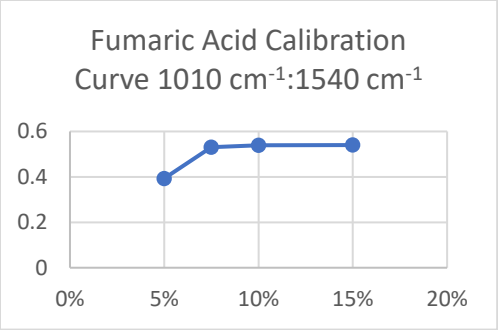

Figure 20 - Calibration curve created using 4 data points. The data points are made from samples created with Fumaric acid and JEJ tissue. Each decreasing percentage value is the result of lower polymer concentration within tissue. The Y axis is generated using specific polymer peak (at 1010 cm^{-1}) versus specific tissue peak (at 1540 cm^{-1}) absorbance ratios. The X axis corresponds to the percentage point of the generated ratio.

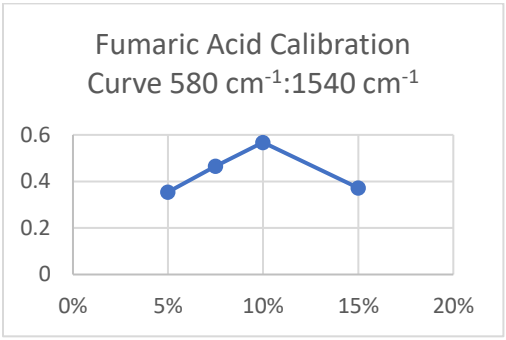

Figure 21 - Calibration curve created using 4 data points. The data points are made from samples created with Fumaric acid and JEJ tissue. Each decreasing percentage value is the result of lower polymer concentration within tissue. The Y axis is generated using specific polymer peak (at 580 cm^{-1}) versus specific tissue peak (at 1540 cm^{-1}) absorbance ratios. The X axis corresponds to the percentage point of the generated ratio.

Blood Plasma Calibration Curve:

As discussed in Aim 1, creating the blood plasma calibration curve involved a different method than the one used in the creation of the GI JEJ tissue calibration curve. The liquid method allowed for more accurate and easier creation of spiked samples, as well as calibration curve points. However, due to the chemical nature of PFASA and its rapid degradation in an aqueous environment, a blood plasma calibration curve using the liquid method could only be made with PLA. Due to the ease of implementing the liquid method, additional points could be made for the PLA blood plasma calibration curve. As seen in Figure 14, the PLA specific peak which stands out the most in the spiked blood plasma sample is at 1750 cm^{-1} wavelength.

Therefore, that peak was chosen as the model peak for the blood plasma calibration curve. The specific peak absorption values used for the calibration curve, as well as the calculated PLA:Blood-plasma peak ratios are given in the table below:

	1750 cm^{-1}	1654 cm^{-1}	1750 cm^{-1}:1650 cm^{-1} ratio
17.5%	0.2492	1.538	0.162029
15%	0.2035	1.384	0.147038
12.5%	0.1831	1.569	0.116699
10%	0.1728	1.662	0.103971
7.5%	0.1308	1.589	0.082316
5%	0.111	1.626	0.068266
2.5%	0.09402	1.835	0.051237
1%	0.0714	1.683	0.042424

Table 6 - Table listing the extracted absorbance data from the PLA blood plasma calibration curve points. The data was extracted using SpectraGryph and was processed in Microsoft Excel. Each column lists the absorbance of the spectrograph at the specific wavelength. Each percentage points corresponds to the percent of PLA in the sample. The remainder of the sample was made from blood plasma. The 1750 cm^{-1} points are attributed to PLA specific peaks while the 1650 cm^{-1} points are attributed to blood plasma specific peaks.

After the blood plasma calibration curve points were extracted from the spectrograph files using SpecrtaGryph, they were transferred to excel. Table 6 lists the peaks of the extracted files. The 1750 cm^{-1} peak was chosen as the PLA specific peak, while the 1650 cm^{-1} peak was chosen as the blood plasma specific peak. As discussed previously, the actual calibration curve points are made up from the PLA:Tissue peak ratio, as well as the percentage that that ratio is tied to. The third column in Table 6 lists the PLA:Blood-plasma ratios. From the calculated ratios, a calibration curve can be made for PLA in blood plasma as can be seen in Figure 22.

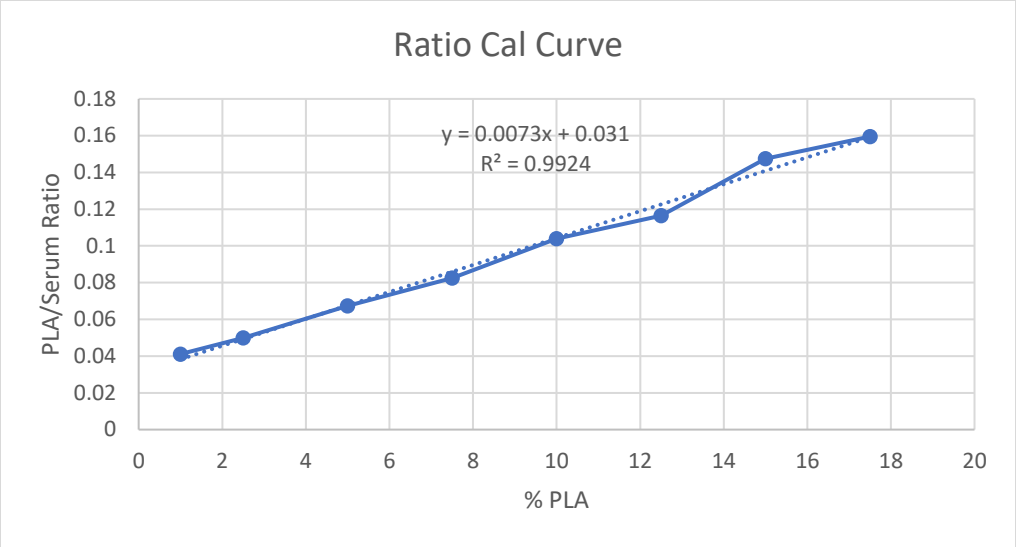

Figure 22 - Calibration curve created using 8 data points. The data points are made from samples created with PLA and blood plasma. Each decreasing percentage value is the result of lower polymer concentration within tissue. The Y axis is generated using specific polymer peak (at 1750 cm^{-1}) versus specific tissue peak (at 1650 cm^{-1}) absorbance ratios. The X axis corresponds to the percentage point of the generated ratio.

The linearity of the calibration curve shown in Figure 22 is due to the accuracy and precision of the liquid method. This method minimizes the possibility of human error, while also limiting the problems which could occur when dealing with low weights, as noted when creating the tissue calibration curves.

Discussion

Several attempts were made to create calibration curves for PLA, PFASA and Fumaric acid. Of all the samples, Fumaric acid showed least promise when creating a curve for JEJ tissue. A calibration curve was successfully created for both PLA and PFASA in JEJ tissue.

From the two calibration curves made of PLA in JEJ tissue, the most promising one is shown in Figure 16. While figure 15 does show a relative downward slope, the inconsistent ratio decrease with a decrease in PLA concentration excludes it from being used in any *in-vivo* experiment. The second PLA concentration curve, which was created with the 1185 cm^{-1} specific PLA peak showed a more consistent downward trend. In fact, this trend is relatively linear until the low

PLA concentrations of 2.5% and lower. The unexpected spike at the PLA concentration of 1% occurred after several repeat attempts to create the same concentration point. The possible explanation as to why the concentration curve becomes inconsistent at the lower concentrations is perhaps a detection limit to the FTIR spectrometer. A second explanation could be that at such low PLA concentrations, it becomes impossible to completely homogenize the polymer within the tissue using a mortar and pestle. If not homogenized, the spectrometer could be reading an area of the pellet sample where no PLA is present. The proposed solution to this problem would be to somehow implement the liquid method used for the blood plasma calibration curve into the GI tissue calibration curve.

Calibration curves were also created for poly-Fumaric-co-Sebacic-acid. Those calibration curves are shown as Figures 17-18. As seen, only Figure 17, a calibration curve using the 1812 cm^{-1} PFASA specific peak, showed a relatively consistent downward trend. The 1812 cm^{-1} peak was chosen in Aim 1 as the most likely candidate to create the PFASA calibration curve. The peak in question is created from an anhydride bond, a relatively unstable bond usually not present in biological tissue without protecting groups. This bond would therefore be lacking from biological tissue and should be used as the PFASA specific peak. The most likely reasoning behind the 7.5%-point spike seen in Figure 17 is the rapid degradation of the anhydride bond. The bond within the 10% sample could have started degrading, lowering its absorbance, and disrupting the linearity of the calibration curve. A possible solution to the problem of spiked points in PFASA calibration curves would be to conduct the experiments in completely moisture free environments and store any PFASA within desiccators to prevent degradation.

An attempt at creating a calibration curve for fumaric acid was made in case a calibration curve for pure PFASA yielded no results. The reasoning behind this decision was that if the

polymer itself could not be detected in tissue or blood due to rapid degradation, perhaps one of the constituents of the polymers, which was more stable, could. As seen in Figueres, 19-21, the sample points made from the Fumaric acid monomer and JEJ tissue yielded no calibration curve. This can be explained by the fact that Fumaric acid had no strong specific peaks lacking in the Tissue samples. And while a calibration curve could not be made using the Fumaric acid monomer, the presence of the monomer could potentially be confirmed. As shown in Figure 11, a definitive change to the sample, as compared to the control, was noticed in the 700-500 cm^{-1} region. The addition and or presence of the two peaks which appear with Fumaric monomer could be used to provide evidence of PFASA uptake and degradation within the GI tissue.

The final calibration curve create was made using PLA and plasma, utilizing the liquid method. The calibration curve created is seen in Figure 22. This calibration curve showed the most consistent downward trend with decreasing PLA concentrations out of any other curve. This can be attributed to the method used to create the curve. Additionally, as seen in Figure 10, there is a slight difference between the blood plasma control and JEJ-WM tissue control samples. This difference manifests as a peak in the 1730 cm^{-1} region of the JEJ tissue control. The presence of this peak could have influenced the 1750 cm^{-1} JEJ tissue calibration curve, while the lack of this peak in the blood plasma control could have helped with the creation of a more consistent downward trend.

In conclusion, the goal of creating calibration curves for the three selected samples, PLA, PFASA and Fumaric acid, resulted in the successful creation of curves for PLA and PFASA. Additionally, the most consistent calibration curve was created using the liquid method, and was made with PLA and blood plasma.

Specific Aim III – Using the created calibration curves to calculate polymer uptake in an in-vivo experiment.

Experimental Section:

December 2017 Experiment:

Once the calibration curves were created, an *in-vivo* experiment could be designed to test the polymer detection and polymer uptake methods used in Aims 1-2. Due to the calibration curve results seen in Aim 2, the polymer chosen to in Aim 3 was PLA. The objective of Aim 3 was to test the results and methods used throughout the first two aims, in order to detect and calculate the percent uptake of PLA in blood plasma.

Initially, a simple *in-vivo* experiment was designed to test the results while sacrificing only one rat, and it was named the December *in-vivo* experiment. The Mathiowitz lab conducted an isolated loop operation, where a large quantity of PLA was fed into the GI of a rat. The rat was maintained for 5 hours, after which it was sacrificed. Blood was collected from the rat at both the 0-hour time point, and the 5-hour time point. The blood was then separated into erythrocytes and blood plasma, as described in the method section of Aim 1. The blood plasma was then analyzed and compared to the 0-hour control and pure PLA spectrographs. The samples, both the 0-hour and the 5-hour, as well as all the standards made for the blood calibration curves were all made with the same 99:1 KBr:Sample concentration. The resulting spectrograph is shown in Figure 23.

October 2018 Experiment:

After it was shown that PLA could be detected in an *in-vivo* experiment using the blood plasma calibration curve, another project was designed to further investigate and confirm those findings.

The second experiment was conducted in a similar fashion as the first. For the confirmation experiment, four rats were sacrificed instead of one. This was done to test the accuracy of the finding, as well as eliminate negative results which could occur due to many different factors. This second *in-vivo* experiment was named the October *in-vivo* experiment.

The preparation for this experiment was much more extensive to minimize any possible data loss. The decision was made to also collect several organs from the rats, which could later be used for detection, once calibration curves for those organs had been made. Blood and GI were also collected from the four rats. A vital step in the preparation for the experiment was to label and pre weigh all the vials to be used, as even slight mislabeling could drastically change the calculated concentrations, and polymer uptake predictions.

The experiment followed the isolated loop procedure commonly used in the Mathiowitz lab. The rats were individually anesthetize using isoflurane and kept warm under heating blankets and also on top of a heating pad set to 37C. 0-h time point blood samples were collected from their tails and placed in 1.5 mL vials. Those vials were left at room temperature for the purpose of clumping. Once 20 minutes passed, the vials were placed on ice.

These vials were labeled as 0-hour vials. The purpose of the 0-hour blood is to create individual baselines for each rat. After being placed on ice, they were transferred to the centrifuged, and the layers separated as described in Aim 1. The plasma layers were then

transferred to other pre-weighed vials, and both the erythrocyte and plasma 0-hour vials were lyophilized for a week.

After the 0-h time point blood samples were extracted from the rats, isolated loops were made from the rat GI, and 100 mg of PLA in DI water was injected into the isolated loop. The rats were kept under anesthesia for 5 hours which was enough time for nanoparticle uptake to occur, as shown in the initial experiment. After taking the 5 hour time point (similarly to the 0-h time point) the rats were euthanized. The 5-hour blood samples were processed in the same way as well. Organs and the GI isolated loops were harvested from the rat. The full list of organs, initial vial weights, and post-harvest vial weights are given in Table 7.

Results and Analysis:

December *in-vivo* Results:

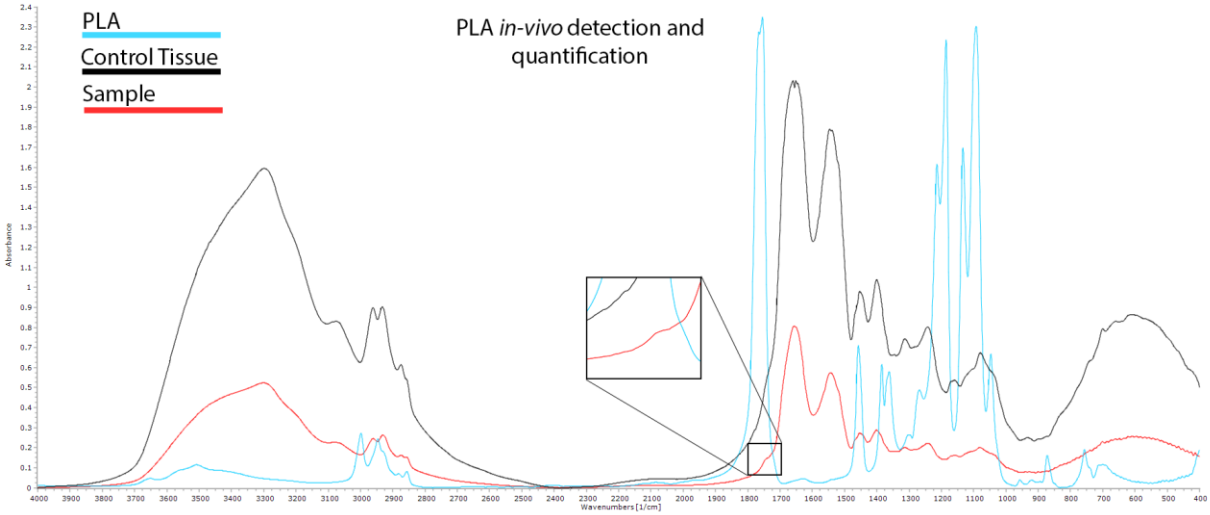

Figure 23 – A spectrograph collected after processing the single rat *in-vivo* experiment. The three colors represent different samples collected: Blue-Pure PLA polymer, Black-Control Plasma collected at the 0-hour time point, and Red-Blood plasma collected from the isolated loop experiment at the 5-hour time point. The magnified region shows a slight bump which was detected in the 5-hour time point, indicating slight PLA absorbance into the rat's blood stream. The figure and analyzed data were baselined and not normalized for the December experiments.

The magnified region (Figure 23) shows a peak indicative of PLA absorption into blood. While the peak itself might not look significant, it still indicates slight PLA presence in the circulating blood stream. The data from the 5-hour time point was extracted into SpectraGryph and transferred into Excel for further analysis.

To determine the percentage of PLA in the spectrograph sample seen in Figure 23, the extrapolated data was compared to the calibration curve (Figure 22) created for blood plasma and described in Aim 2. The peak data gathered from the *in-vivo* experiment differed slightly from the general data gathered in the *ex-vivo* experiments done throughout Aim 1-2. Specifically, the blood plasma peak at 1650 cm^{-1} was lower than that of the spiked and controlled peaks (Figure 14) collected thus far. This inconsistency resulted in the PLA:Blood peak ratio being much greater than expected. For the December rat, when comparing the extracted data from the *in-vivo* experiment with the calibration curve (Figure 22) made in Aim 2, the PLA concentration in blood plasma of the pellet sample results in 17.95%. In this calculation (which is not the final correct one) we did not subtract the 0 hour time point from the 5 hour time point, which would reduce the PLA concentration in blood plasma. Because the blood plasma peak from the in-vivo sample was low, I wanted to compare the blood plasma peaks of other rats to the *in-vivo* one. To do this, I averaged all the blood plasma peaks of the standards used to create the calibration curve and used that value for the analysis of the December rat. This resulted in a PLA concentration of 6.83%, like what will be calculated with the Pure Absorbance Curve.

To evaluate the peak height alone for the December rat, and minimize the error seen from the unusually low blood plasma peak, a second calibration curve was created. Instead of using the PLA peak to Blood plasma peak ratios to generate the calibration curve points, the second curve was made from pure PLA-specific peak absorbance heights. Because this curve is made

from purely the absorbance peak heights, it was named the Pure Absorbance Calibration Curve. The curve is shown in Figure 25.

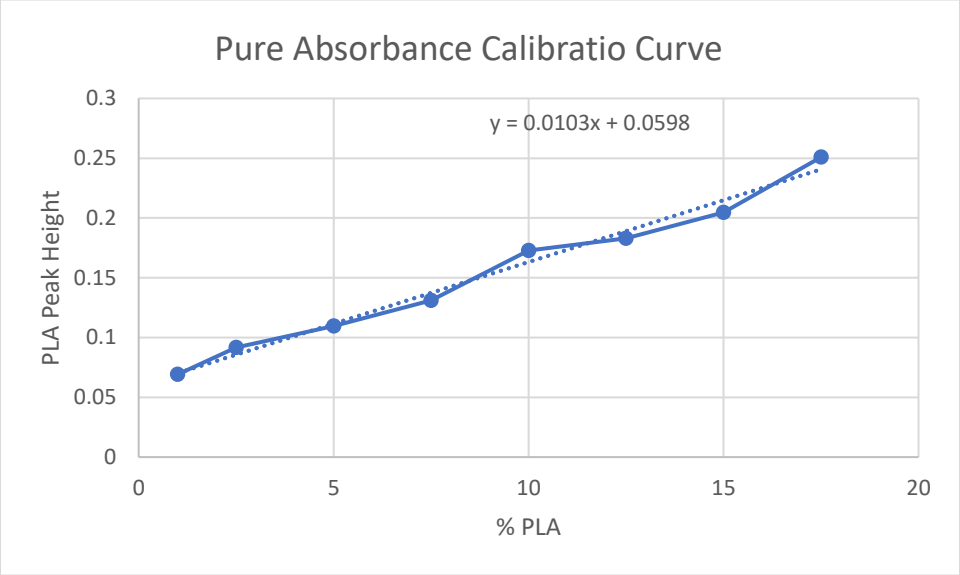

Figure 24– A calibration curve made from the same data points as the curve shown in Figure 22. Unlike the calibration curve in Figure 22 which was made from the PLA:Blood absorbance peak ratios, this calibration curve was made from the PLA-specific peak heights alone. The equation for the calibration curve line is given in the figure. The standards which were used to make the calibration curve and the samples which were analyzed were all processed in the same way. This includes making the pellet concentration 99:1 KBr:Sample, baselining and normalization.

After the second calibration curve was made, the peak absorbance from Figure 23 was used to determine the PLA concentration in the *in-vivo* experiment. The PLA concentration calculated using the curve shown in Figure 25 was 6.885%, as opposed to the 17.951% calculated from the ratio calibration curve shown in Figure 22.

Knowing the percentage of PLA in plasma, we were then able to calculate the total amount of PLA in the blood. First, the standard way of determining the total blood volume in rats is to use the 5.7 mL per 100g ratio (Schreihofer et al). This resulted in much higher uptake (over 100%) of PLA in our *in-vivo* model for the December rat. However, additional research showed that obese rats contain lower blood volumes per 100 g, and a ratio of 3.4 mL per 100 g could be used instead (Schreihofer, et al). Knowing that our rat weighed 766 g, this would result

in a total blood volume of 24.5 or 25 mL using the 3.4 mL per 100 g ratio. Additionally, since our FTIR samples need to be in a dry form to process and analyze, all the blood and plasma was lyophilized. We lyophilized the blood before measuring the exact volume collected. This resulted in a problem because we were unaware of how much blood volume translated into plasma volume, and subsequently plasma mass in grams. To solve this, we conducted another experiment where we collected rat blood in 1 mL vials, centrifuged them to separate the erythrocytes from plasma, transferred the top (plasma) layer into separate vials, and lyophilized both layers. Doing this allowed us to determine that 1 mL of blood contains an average of 42 ± 7.2 mg of dried plasma. Knowing that the *in-vivo* rat contained 25 mL of blood, and that 1 mL of blood contains 42 mg of plasma, then the total plasma within this rat equals 1029 mg. From the total plasma, our calibration curves show that 6.8% is PLA, resulting in 70 mg of PLA being detected in blood. Knowing that 84.6 mg of PLA was the administered dosage in the isolated loop experiment, and that 70 mg was detected using the calibration curve, the total PLA uptake from the December experiment was 82.7%. The calculations within this paragraph are shown below:

Determining PLA % using Cal. Curve:

In-vivo PLA peak value: 0.130, *In-vivo* Tissue Peak value: 0.806, *In-vivo* PLA:Tissue peak Ratio: 0.162

Pure PLA peak Calibration Curve Equation:

y = 0.0103x + 0.0598 -> 1.30 = 0.0103x + 0.0598 -> x = 6.8835 (% of PLA in sample)

PLA:Tissue ratio Calibration Curve Equation:

y = 0.0073x + 0.031 -> 0.080 = 0.0073x + 0.031 -> x = 6.83064 (% of PLA in sample)

Rat blood volume calculations:

Rat weight: 766 g, Total blood volume = (766/100)*3.2 mL = 24.512 mL

Total grams of Plasma per 1 mL of blood: 42 g/mL.

Total grams of Plasma for December *in-vivo* rat: 25 mL * 42 g/mL = 1029 g

Plasma Uptake calculations:

Total PLA injected during *in-vivo* experiment: 84.6 g

Amount of PLA in blood: Total blood Plasma x PLA % ->

-> 1029 g x 6.8% = 70 g of PLA in Rat blood

Percent of PLA uptake: $\frac{Bioavaliable\ PLA}{Total\ PLA\ injected}\ x\ 100\% = \frac{70\ g}{84.6\ g} x\ 100 = 82.7\%$

It should be mentioned that the same method for calculating bioavailability was applied to all *in-vivo* rat experiments used in this project. The differences are only in the calibration curves used to calculate PLA concentrations in blood plasma, analysis method, and sample values obtained for each individual rat.

October *in-vivo* experiment Results:

The tables below list all the collected data for the October *in-vivo* experiments. Specifically they list all the organ weights and blood volumes and weights for the four rats used in the experiment. Organs weren't analyzed for this project.

	Rat 1	Rat 2	Rat 3	Rat 4	December Rat
Weight (grams)	367	270	450	510	766
Total blood volume (mL)	20.9	15	15	17	26
Total plasma weight (mg)	878.3	646.2	642.4	728.1	1093.5

Table 7 – Table listing the weights of all the rats used in the two in-vivo experiments. Rats 1-4 were weighed before the October in-vivo experiments, and the December Rat was weighed before the December in-vivo experiment. Additionally, the table lists the total blood volume of the five rats, and the total plasma weight. The blood volume is generated from the ratio of 3.4 ml/100 g for normal weight rats (under 400g) and 5.7 ml/100 g for obese rats (over 400g). The total plasma weight was gained form the ratio of 42 mg/mL of blood which was calculated within the Mathiowitz lab.

W/Cap	Rat 1	Rat 2	Rat 3	Rat 4
Liver	14807.9	14861.7	14864.7	14859.8
Spleen	14801.1	15169.9	15009.9	14983.2
IL	15100.4	14961.2	14867.9	14813.3
Heart	14947.4	14779.7	14898.3	14820.8
Lungs	14860.1	14795.9	14977.2	14954.3
Kidneys	14815.7	14864.6	14936.6	14902

Table 8 – Table listing the initial vial weights for the four rat in-vivo experiment. The weights are given in mg.

W/Cap	Rat 1	Rat 2	Rat 3	Rat 4
Liver	17029.3	17096.3	18375.38	18938.7
Spleen	14936.68	15265.7	15162	15193.85
IL	15371.1	15351.6	15303.8	15383.09
Heart	15388.2	15009.31	15209.6	15171.76
Lungs	15059.7	15066.46	15538.7	15393.03
Kidneys	15693.19	15588.1	15857.46	16035.8

Table 9 – Table listing the vial weights after organ deposition. The weights are given in mg.

W/Cap	Rat 1	Rat 2	Rat 3	Rat 4	Averege
Liver	2221.4	2234.6	3510.68	4078.9	3011.395
Spleen	135.58	95.8	152.1	210.65	148.5325
IL	270.7	390.4	435.9	569.79	416.6975
Heart	440.8	229.61	311.3	350.96	333.1675
Lungs	199.6	270.56	561.5	438.73	367.5975
Kidneys	877.49	723.5	920.86	1133.8	913.9125

Table 10 – Table listing the individual weights of the organs collected. The number was gained by subtracting the vial weight with sample values from the pure vial weight values. The weights are given in mg.

Blood	Rat 1	Rat 2	Rat 3	Rat 4
0 Hr Plasma	458.4	456.8	456.0	453.5
0 Hr Erythrocyte	456.7	457.11	459.8	458.7
5 Hr Plasma	1017.9	1019.8	1016.88	1031.7
5 Hr Erythrocyte	1019.4	1031.32	992.12	1017.8

Table 11 – Table listing the initial vial weights used to collect the blood samples at the 0-hour and 5-hour time points. The weights are given in mg.

Blood	Rat 1	Rat 2	Rat 3	Rat 4
0 Hr Plasma	477.5	476.4	470.2	470.8
0 Hr Erythrocyte	532.1	547.9	563.8	559.2
5 Hr Plasma	1064.3	1063.2	1050.3	1060.9
5 Hr Erythrocyte	1160.6	1207.5	1158.2	1199.3

Table 12 – Table listing the vial weights of the 0-hour and 5-hour samples after they were collected, separated and lyophilized. The weights are given in mg and relate to the pure dry mass of the samples collected.

Blood	Rat 1	Rat 2	Rat 3	Rat 4	Average
0 Hr Plasma	19.1	19.6	14.2	17.3	17.55
0 Hr Erythrocyte	75.4	90.79	104	100.5	92.6725
5 Hr Plasma	46.4	43.4	33.42	29.2	38.105
5 Hr Erythrocyte	141.2	176.18	166.08	181.5	166.24

Table 13 – Table listing the pure weights of the 0-hour and 5-hour samples collected. The weights are given in mg and relate to the pure dry mass of the samples after they were separated and lyophilized. The values were calculated by subtracting the pure vial weights from the vial weights containing the samples.

Once the isolated loop experiment was completed, the data needed to be processed and analyzed. The first step in this process was to create FTIR spectrometer blood plasma pellets. To do so, 1 mg of the 0-hour time points were weighed out and transferred to the non-electrostatic mortar. To the blood plasma samples, 99 mg of KBr was added and mixed until homogenous, the same ratio as was used for the blood calibration curve. Once the mixing was complete, 100 mg of the sample was pressed for 15 min at 10,000 kg force. This process was completed for all four control (0-h time points) samples. The same process was done for the four 5-hour time points. All the pellets were then scanned in the FTIR spectrometer. The spectrograph files were exported to SpectraGryph for further analysis.

The first step of the analysis was to identify possible PLA specific peaks within the 5-hour time points. To do so, the control 0-hour time point was compared to the respective 5-hour sample for peak detection. Specifically, the main objective was to analyze the region where the PLA specific peak usually manifests, which is the 1750-1730 cm^{-1} region. The detection and

quanitifcation of PLA in the samples from the October *in-vivo* experiment differ from the methods used in the December *in-vivo* experiment. First, detection in the previous method (used in the December experiment) was done through a qualitative process, where a peak bump alone confirms PLA presence. This new method confirms detection by a quantitative process, where if a subtraction of the 0 hour time point PLA peak from the 5 hour time point PLA peak results in a positive value, PLA presence is confirmed. Negative or null values after subtraction are considered a non-uptake. Once PLA presence is confirmed, additional steps can be taken to quantify the concentration and systemic uptake (bioavailability) of PLA in the body. Figures 26-29 depict the spectrographs of the 5-hour samples overlaid with the 0-hour control and pure PLA spectrographs for comparison. Where applicable, a zoomed in depiction is present to better show the PLA specific peak bump.

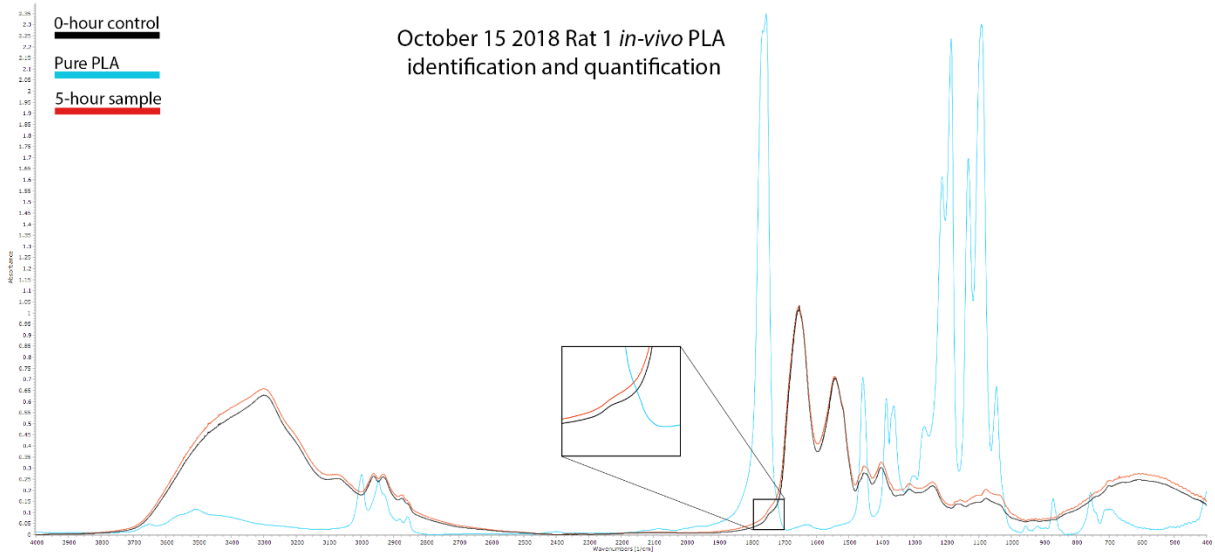

Figure 25 - A spectrograph collected after processing the first rat from the October *in-vivo* experiment. The three colors represent different samples collected: Blue-Pure PLA polymer, Black-Control collected at the 0-hour time point, and Red-Blood plasma collected from the isolated loop experiment at the 5-hour time point. The magnified region shows a slight bump which was detected in the 5-hour time point, indicating slight PLA absorbance into the rat's blood stream. When conducting the analysis, the FTIR samples were baselined and normalized. The pellet concentration was 99:1 KBr:Sample.

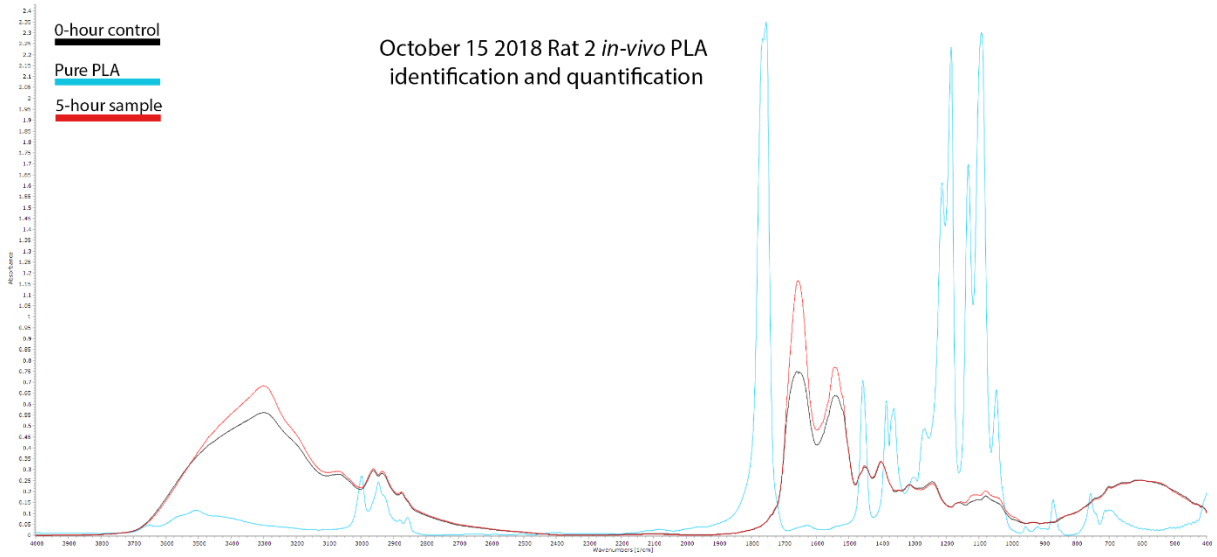

Figure 26- A spectrograph collected after processing the second rat from the October *in-vivo* experiment. The three colors represent different samples collected: Blue-Pure PLA polymer, Black-Control collected at the 0-hour time point, and Red-Blood plasma collected from the isolated loop experiment at the 5-hour time point. Since no PLA specific peak was detected in this rat, a magnified region for this spectrograph was not made. When conducting the analysis, the FTIR samples were baselined and normalized. The pellet concentration was 99:1 KBr:Sample.

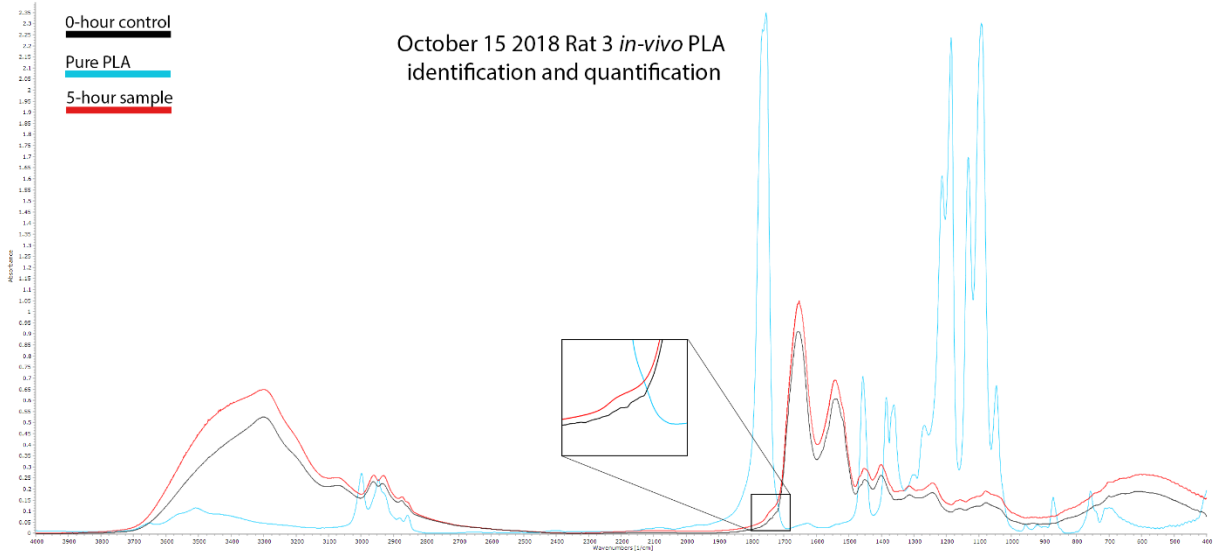

Figure 27 - A spectrograph collected after processing the third rat from the October *in-vivo* experiment. The three colors represent different samples collected: Blue-Pure PLA polymer, Black-Control collected at the 0-hour time point, and Red-Blood plasma collected from the isolated loop experiment at the 5-hour time point. The magnified region shows a slight bump which was detected in the 5-hour time point, indicating slight PLA absorbance into the rat's blood stream. When conducting the analysis, the FTIR samples were baselined and normalized. The pellet concentration was 99:1 KBr:Sample.

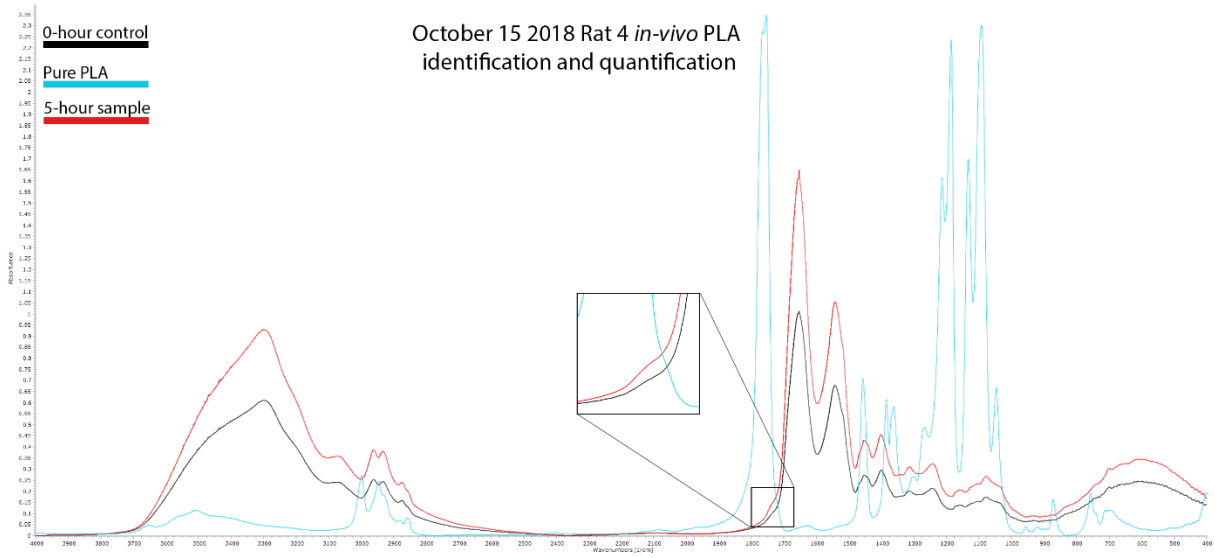

Figure 28 - A spectrograph collected after processing the fourth rat from the October *in-vivo* experiment. The three colors represent different samples collected: Blue-Pure PLA polymer, Black-Control collected at the 0-hour time point, and Red-Blood plasma collected from the isolated loop experiment at the 5-hour time point. The magnified region shows a slight bump which was detected in the 5-hour time point, indicating slight PLA absorbance into the rat's blood stream. When conducting the analysis, the FTIR samples were baselined and normalized. The pellet concentration was 99:1 KBr:Sample.

As shown in Table 15, two rats from the 4 tested in the October *in-vivo* experiment didn't show PLA within blood plasma. The other two rats (termed Rat 1 and Rat 3) showed positive values when subtracting the 0-hour PLA peak from the 5-hour PLA peak. This indicates that PLA was present in the blood of those rats. As such it can be concluded that PLA nanoparticles penetrated through the GI within the isolated loop experiment. Additionally, since the PLA was found in blood, it can be concluded that the nanoparticles were then absorbed into the blood stream once they penetrated through the GI.

After detecting PLA within blood plasma, the next step was to quantify the concentration of PLA within the samples, and from that calculate the percent of PLA which successfully entered the blood stream. To do this, an updated calibration curve was made. This curve contained 3 repetitions for each percentage point, while the original contained only one. Additionally, the calibration curve was made by the 0% PLA sample (blood plasma only) from each percentage point. This ensures that any increase in absorption within the sample results

mainly from the addition of PLA within the sample. These two steps were taken to make the calibration curve more precise and accurate. Once the spectrographs were obtained, they were baselined and normalized. Normalization of the spectrograph resulted in the plasma peak height always equaling one because it was the highest peak in the spectrograph. Because the plasma peaks equal one, ratio calculations were not needed to be done in excel, as it would result in any PLA peak being divided by one.

When calculating the concentration of PLA within blood for each rat, the 0-hour control was subtracted from the 5-hour sample, which should minimize any errors, and again ensure that any increase in absorption is a direct result of PLA within the blood stream. All the quantification steps were done in Excel. The calibration curve points which were used to create the third calibration curve are given below.

Percent	1750 cm^{-1}	Mean
	0.05015	0.04802
1%	0.04476	
	0.04915	
	0.0539	0.053353
2.50%	0.05141	
	0.05475	
	0.08983	0.083237
5%	0.07836	
	0.08152	
	0.1137	0.1154
7.50%	0.1227	
	0.1098	
	0.1563	0.144267
10%	0.1396	
	0.1369	
	0.1622	0.166167
12.50%	0.1562	
	0.1801	
	0.2051	0.203433
15%	0.2127	
	0.1925	

Table 14 – Table listing all the calibration curve points used to create the second PLA blood plasma calibration curve. Each point on the curve is created using three data points. These points are then averaged to create a single percentage point which is subsequently used to create the calibration curve. The calibration curve has a range from 1-15% PLA. The first column lists the concentration of PLA in blood used to create the sample, the second lists the three individual points created using said concentration, and the third column lists the averages of the three points in the same concentration bracket.

Once the calibration curve points were extracted from SpectraGryph, and processed in Excel, a curve shown in Figure 30 was generated.

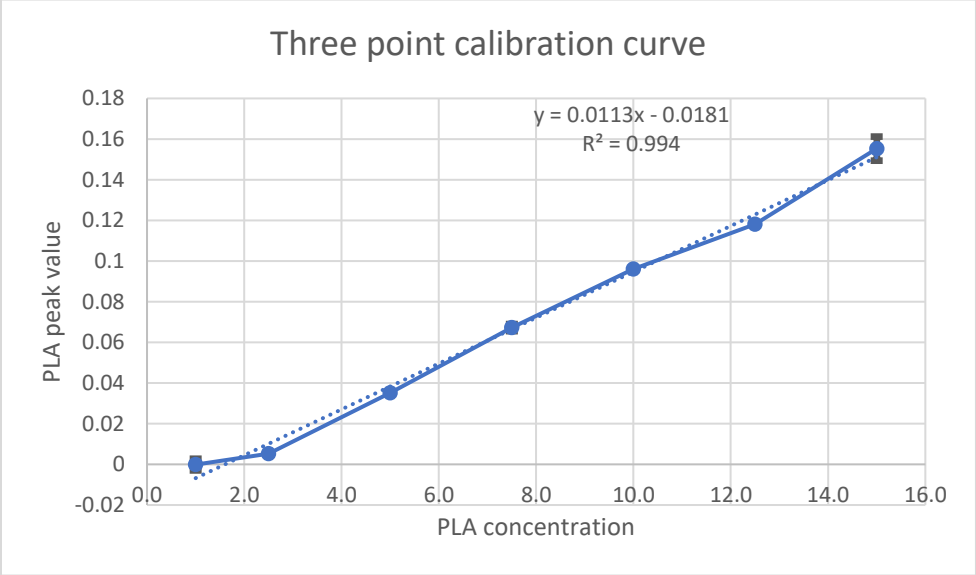

Figure 29 - calibration curve generated for PLA using blood plasma. The curve was generated from the data points shown in Table 13. The curve has a percentage range from 1-15%. Each point is generated from an average of three distinct sample points. The X axis represents the concentration of PLA at the sample from which the point was gathered. The Y axis represents the PLA:Blood peak ratio. When making the curve the spectrographs were linearly baselined and normalized.

After PLA was identified as present in the blood of rats one and three, the absorbance of the PLA peak was collected in SpectraGryph. The data was Exported into excel to analyze against the calibration curve shown in Figure 30.

	Rat 1	Rat 2	Rat 3	Rat 4
5-hour	0.1139	0.0721	0.09078	0.07556
0-hour	0.08871	0.1046	0.06546	0.08567
Absolute Absorbance	0.02519	-0.0325	0.02532	-0.01011
PLA Concentration	3.83879	0	3.85031	0

Table 15– Table which shows the absorbance data gained from the October in-vivo experiment. The first row lists the absorbance values of 0-hour control from each rat, extracted from the point where the PLA peak is generally seen. The second row lists the absorbance values of the 5-hour sample from each rat, collected from the visible PLA peak. The third row is generated by subtracting the 0-hour absorbance peak from the 5-hour absorbance peak.

Table 15 lists the absorbance data collected from the three *in-vivo* rats which showed a peak at the PLA specific region (Figures 26-29). The 0-hour absorbance data was also collected

to act as a baseline for the 5-hour sample. After subtracting the 0-hour baseline from the 5-hour sample, PLA was detected in Rats 1 and 3. As seen in Table 14, Rats 2 and 4 had negative values post subtraction, and as such there was no detection of PLA within the blood of these rats.

Once the *in-vivo* rat spectrographs were baselined and normalized, it was plugged into the third calibration curve shown in Figure 30. PLA concentration within each sample was calculated using the generated calibration curve. Because the 5-hour sample pellets represent the circulating blood at that time point, it can be concluded that the PLA concentration within the pellets corresponds to the PLA concentration within the circulating blood plasma. Table 15 lists the PLA concentrations in blood plasma for rats in which PLA was detected.

As explained in the December experiment, one can estimate the total blood volume of a rat by knowing its weight. A ratio of 3.4 mL / 100 g is used for rats which are obese, while a ratio of 5.7 mL / 100 g is used for non-obese rats. After the total blood volume of each rat was calculated, the total weight of blood plasma could then also be calculated. Using previous experiments and data collected, 1 mL of blood results in approximately 42 ± 7 mg of blood plasma. Knowing the concentration of PLA in blood plasma, we were then able to calculate the total mass of PLA in the circulating blood. After calculating the total mass of PLA in blood using the steps described above, we were then able to calculate percent of systemic uptake using the known amount of PLA within the circulating blood versus the known amount of PLA injected into the rats. The table which lists the results of all the calculations for each individual rat is given below:

	Weight (g)	Dosage (mg)	Left over (mg)	Actual dosage (mg)	Total Blood volume (mL)*	Total Plasma mass (mg)***	Uptake (%)
Rat #1 (F)	367	110.2	19.2	91	20.9	878.3	37
Rat #3 (M)	450	110.4	43.9	66.5	15	642.4	37

Table 16 – Table showing the values gained in the process of calculating the percent total bio-uptake of PLA in the two viable rats from the October in-vivo experiment. The first column represents the total weight of each rat. This was used to estimate the total blood volume of each rat. The second column represents the total dosage of PLA loaded into the syringe to be injected into the isolated loop. The third column represents the leftover from the injection still available in the syringe. The fourth column represents the actual amount of PLA which was injected into the rat in question (Dosage-Leftover). The fifth column represents the total blood volume of the rat. The sixth column represents the total mass of dried blood plasma available in the rat (42mg/ml of blood). The seventh column represents the percent biouptake of PLA in the circulating blood.

Table 15 shows the result of the *in-vivo* October experiment. As previously discussed, the purpose of the third Aim was to use the knowledge and data gained from Aims 1 & 2 and apply them to a live experiment. The third aim was designed to test the applicability of an FTIR based polymer:tissue calibration curve in a more dynamic experiment..

As the method used for the October rats proved to be more consistent, the December rat data was reanalyzed using the new method. This new method includes both the detection by quantification and the biouptake calculation by the third calibration curve. The new calculations and reanalyzed samples are listed below:

0 h	0.1586
Sample (5h)	0.1785
Absolute	0.0199
Calc Percent	**3.36**

Table 17 – Table showing the absorbance values of the December rat after re-analysis. The calculated percentage represents the PLA concentration in the sample gained using the new method and the third calibration curve. The samples were normalized and baselined for analysis.

	Weight (g)	Dosage (mg)	Total Blood volume (mL)*	Total Plasma mass (mg)***	Uptake (%)
December Rat	766	84.6	26.044	1093.848	43.4

Table 18 – Table showing the values gained in the process of calculating the percent total bio-uptake of PLA in the December in-vivo experiment. The first column represents the total weight of each rat. This was used to estimate the total blood volume of each rat. The second column represents the actual amount of PLA which was injected into the rat in question (Dosage-Leftover). The third column represents the total blood volume of the rat. The fourth column represents the total mass of dried blood plasma available in the rat (42mg/ml of blood). The fifth column represents the percent biouptake of PLA in the circulating blood.

Ultimately, out of the 5 total rats which were used in the two *in-vivo* experiments, detraction and quantification was applicable in 3 rats. Rats 1 and 3 from the October experiment, and the single rat from the December experiment all showed PLA presence within blood plasma. Additionally, the same rats were also used to successfully quantify PLA uptake into the circulating blood. The samples collected from Rat 2 and 4 in the October *in-vivo* experiment did not show any PLA presence and therefore no steps were taken to calculate the percent systemic uptake of that rat.

Discussion

The entire project to create a method for detecting polymer presence using an FTIR was designed to build upon the success of each previous aim. The initial aim was to use an FTIR spectrometer to broaden the spectrum of detectable polymers in tissue based on the initial research done by the Mathiowitz lab. This was done by successfully identifying poly-lactic acid, poly-fumaric-co-sebacic acid, and fumaric acid in GI tissue. Additionally, the project expanded the possible organs where the polymers could be detected from only GI tissue into blood as well. After successfully detecting the polymers, an attempt was made to create calibration curves for the same polymers in GI tissue, and PLA in blood. No blood calibration curves were made for PFASA and Fumaric acid because they degrade rapidly in aqueous environments, as discussed previously. The calibration curves were successfully created for PLA in GI tissue and Blood, as

well as PFASA in GI tissue. Finally, building upon all the success of the previous steps, two *in-vivo* experiments were designed to test the feasibility of both detecting and quantifying PLA in the blood a live rat model.

The steps taken to conduct the *in-vivo* experiments are described in the **October *in-vivo* experiment** and **December *in-vivo* experiment** sections. The result of the experiments was the successful detection of PLA in three of the five tested rats, and a successful biouptake calculation for three of the five rats. Additionally, as described in those sections individually, the two rats from the October *in-vivo* experiment had extremely similar biouptake percentages, which could indicate high precision for the calibration curve created. The rat from the December *in-vivo* experiment showed different levels of biouptake, partially due to the abnormality seen in its tissue specific peak (using calibration curves 1 and 2). The peak itself wasy low, as compared to the standards used to create the calibration curve as well as the October *in-vivo* samples. The lower than normal tissue peak skewed the uptake percentages higher than what could be expected. However, once the detection and biouptake methods form the October experiment were applied (using calibration curve 3) to the December experiment, PLA concentration in blood plasma and biouptake percentages were more in line with the values gained from the October experiment.

The only rats where no PLA was detected, and therefore no biouptake calculated were the labeled Rats 2 and 4. The most likely explanation for this outlier has to do with the isolated loop experiment itself. During the process of segregating a section of the GI where the PLA is to be injected, the tract needs to be isolated from the upstream and downstream regions of the GI. To do so, a thin suture is used to tie off each end of the isolated loop. The suture itself is very thin and can therefore tear the GI tract easily. During the process of creating the isolated loop for Rat

2, the top end of the loop cut through the tissue. This resulted in blood pooling within the isolated loop over the five hours during which the rat was kept alive. The presence of blood within the isolated loop could have prohibited the successful absorption of PLA nanoparticles into the epithelium, and therefore altered the results of the experiment. This explanation is most likely the reason as to why no PLA was detected within the circulating blood stream.

Future Discussions:

While the goal set out at the start of the project was carried out to completion, the process of completing it revealed several issues which should be discussed for the benefit of future research into this topic. The process of detecting polymers in any tissue using an FTIR spectrometer can be tricky for several key reasons. A prominent issue is the similarity between the functional groups present on the polymer, and the functional groups present in most biological tissue. As detection of polymer in tissue depends on the formation of an FTIR peak unique to a polymer, the broad range of peaks present on a pure tissue spectrograph limits the available region where a polymer specific peak could occur. Additionally, because polymers selected for human consumption need to be biodegradable and nontoxic, the available selection of polymers which would be tested using the FTIR detection method is even more limited. The polymers which fit this narrow definition of being biodegradable and nontoxic tend to share many functional groups present in tissue, which is another limiting factor for detecting a pure polymer peak. Additionally, the viability of detecting polymers in tissue could be limited by the difference between spectrographs of two separate tissue samples. As Figures 4 and 5 show, there is a difference between the spectrograph images of pure JEJ GI tissue and that of blood plasma. This difference is the main reason as to why a calibration curve for PLA using the 1750 cm^{-1}

region resulted in a better calibration curve for blood plasma, as compared to GI tissue which shows a peak in a nearby region (comparing calibration curves Figures 15 and 25). This means that while a polymer could be detected in one form of tissue, it might not be detectable in another. Taking these considerations into account, the general guideline that was used when selecting the polymers for this project was to pick those which contained easily hydrolysable functional groups. As most tissue contains large quantities of water, hydrolysable functional groups would degrade rapidly in tissue. Therefore, these functional group, while most likely present in tissue, would be of very low concentration compared to other functional groups, and as such would most likely not show up on an FTIR spectrograph. This would then free several regions for polymer specific peaks to appear on, without the influence of tissue peaks.

Additional issues arose when creating calibration curves for the different polymers, some of which could use more development. The initial calibration curves that were made relied on the method previously developed in the Mathiowitz lab. This technique involves grinding GI tissue, polymer and KBr in a non-electrostatic mortar to create a spectrometer ready sample. Since GI tissue is very elastic and sticky, this method came with difficulties where the sample would stick to the mortar, needing to be scraped off, which could potentially lead to an unequal mixing of tissue and polymer. To improve the chance of equal mixing, the process of scraping and grinding was repeated five times for each sample, which resulted in a time-consuming process where each sample would take anywhere from one to one and a half hours to make. As shown in Figures 15 and 16, even with additional steps taken to ensure equal mixing and precise sample measuring, the concentration curves were less than ideal. To overcome these difficulties, the new liquid method was created to form the blood plasma calibration curve, which yielded a more linear concentration curve with a much better R^2 value (shown as Figure 25). Therefore, when creating

future calibration curves for tissue samples which can be dissolved in water, the liquid method would most likely yield the better calibration curve. Additional development should done to create a better method for the formation of concentration curves which are made from GI tissue samples.

The two *in-vivo* experiments mainly yielded the expected results. However, some topics from Aim 3 could be further discussed. First, only the blood plasma calibration curve was used to verify PLA presence and calculate percent uptake. The JEJ GI tissue calibration curve was not used to calculate PLA concentration in tissue, nor were the JEJ samples used to verify the presence of PLA in GI tissue. The GI tissue samples collected from the four rats in the October experiment contained high levels of oil, even after being lyophilized for a week. This made it extremely difficult to form crystalline pellets necessary for the FTIR spectrometer. As such the samples themselves were extremely difficult to process and read. The most likely explanation is that these four rats were severely overweight, and that not enough fat was excised from the GI tract post excision. The fat turned the samples oily and limited the viability of forming the spectrograph ready pellets. After several attempts, the pellets were successfully formed, but the spectrograph image showed severely distorted peaks from which no useful data could be collected. Therefore, the JEJ tissue samples could not be used to verify PLA presence, nor could the JEJ GI calibration curve be used to calculate the concentration of PLA within the epithelium. Additionally, steps could be taken to see if PLA is detectable in liver tissue, and if so, create a calibration curve for PLA in liver. As shown in the *in-vivo* experiments, PLA readily enters the circulating blood stream, and as such some should end up in the liver. A liver specific calibration curve, in addition to a blood and GI tissue calibration curves could be enough to do a mass balance of PLA, and perhaps evaluate the biodistribution of the nanoparticles.

General Conclusion:

The introduction section clearly defined the goals set out for the entire project. The three basic aims, which build upon each other were the identification of new polymers in GI tissue and blood using an FTIR spectrometer, the creation of calibration curves for the aforementioned polymers in GI tissue and blood, and the practical application of the previous aims through the use of an *in-vivo* experiment. The first aim was successfully completed by the addition of PLA, PFASA and Fumaric acid to the library of polymers which could be detected in GI tissue using an FTIR spectrometer. Additionally, PLA was successfully identified within blood plasma, expanding the possible tissues in which polymers could be detected to blood, as well as GI tissue.

Calibration curves for PLA and PFASA in GI tissues were made, as discussed in Aim 2. Additionally, an attempt was made to create a Fumaric acid calibration curve in GI tissue, which was unsuccessful. PFASA calibration curves were not used because no *in-vivo* experiment using PFASA has been conducted. PLA in GI tissue calibration curves were not used in either the December nor October *in-vivo* experiments, as discussed in future discussions.

Three blood calibration curves were made to test the different methods of detectgion and quantification. Ultimately, the optimal method which was chosen as the final method was to the subtraction method analysis using the third calibration curve (Figure 30). Briefly, this method consists of creating FTIR pellets with a 99:1 KBr:sample ratio, linear baselining and normalizing the spectrographs. The calibration curve was made by subtracting the 0% PLA peak from each percentage point standard. The samples were processed by subtracting the 0-hour PLA peak from the 5-hour PLA peak. The sample Δ was then plugged into the calibration curve to give the PLA concentration in dry blood plasma. Due to the spectrographs being normalized, PLA peak height

equals the PLA:tissue ratio. The calculation for the biouptake was done by translating the PLA concentration in dried plasma to the total amount of PLA in circulating blood and comparing it to the administers PLA dose.

References

Furtado, Stacia et al. "Oral Delivery Of Insulin Loaded Poly(Fumaric-Co-Sebacic) Anhydride Microspheres". *International Journal Of Pharmaceutics*, vol 347, no. 1-2, 2008, pp. 149-155. *Elsevier BV*, doi:10.1016/j.ijpharm.2007.06.039.

Hans, M.L, and A.M Lowman. "Biodegradable Nanoparticles For Drug Delivery And Targeting". *Current Opinion In Solid State And Materials Science*, vol 6, no. 4, 2002, pp. 319-327. *Elsevier BV*, doi:10.1016/s1359-0286(02)00117-1.

Lu, Yifeng et al. "Response To Comment On "Uptake And Accumulation Of Polystyrene Microplastics In Zebrafish (Danio Rerio) And Toxic Effects In Liver"". *Environmental Science & Technology*, vol 50, no. 22, 2016, pp. 12523-12524. *American Chemical Society (ACS)*, doi:10.1021/acs.est.6b04379.

Mathiowitz, Edith et al. "Biologically Erodable Microspheres As Potential Oral Drug Delivery Systems". *Nature*, vol 386, no. 6623, 1997, pp. 410-414. *Springer Nature*, doi:10.1038/386410a0.

Morishita, Mariko, and Nicholas A. Peppas. "Is The Oral Route Possible For Peptide And Protein Drug Delivery?". *Drug Discovery Today*, vol 11, no. 19-20, 2006, pp. 905-910. *Elsevier BV*, doi:10.1016/j.drudis.2006.08.005.

Paragkumar N, Thanki et al. "Surface Characteristics Of PLA And PLGA Films". *Applied Surface Science*, vol 253, no. 5, 2006, pp. 2758-2764. *Elsevier BV*, doi:10.1016/j.apsusc.2006.05.047.

Perez, James. "Designing A Novel Approach To Quantify Polymeric Nanoparticle Absorption". Brown University, 2017.

Schreihofer, Ann M. et al. "Reduced Plasma Volume And Mesenteric Vascular Reactivity In Obese Zucker Rats". *American Journal Of Physiology-Regulatory, Integrative And Comparative Physiology*, vol 288, no. 1, 2005, pp. R253-R261. *American Physiological Society*, doi:10.1152/ajpregu.00498.2004.